Plant Molecular Biology **48:** 767–790, 2002.

A high-density cytogenetic map of the *Aegilops tauschii* genome incorporating retrotransposons and defense-related genes: insights into cereal chromosome structure and function

Elena Boyko[1], Ruslan Kalendar[2], Victor Korzun[3], John Fellers[4], Abraham Korol[5], Alan H. Schulman[2,6] and Bikram S. Gill[1,*]

[1]*Wheat Genetics Resource Center, 4024 Throckmorton Plant Sciences Center, Kansas State University, Manhattan, KS 66506-5502, USA (*author for correspondence; e-mail bsg@ksu.edu);* [2]*Institute of Biotechnology, University of Helsinki, Plant Genomics Laboratory, Viikki Biocenter, P.O. Box 56, Viikinkaari 6, 00014 Helsinki, Finland;* [3]*Institute of Plant Genetics and Crop Plant Research, Correnstrasse 3, 06566 Gatersleben, Germany;* [4]*USDA-ARS, Plant Science Unit, Kansas State University, Manhattan, KS 66506-5502, USA;* [5]*Institute of Evolution, University of Haifa, Mount Carmel, Haifa 31905, Israel;* [6]*Crops and Biotechnology, Agrifood Research Finland, Myllytie 10, 31600 Jokioinen, Finland*

Received 5 April 2001; accepted in revised form 7 September 2001

Key words: bread wheat, microsatellites, molecular genetic map, negative and positive interference, resistance and defense-response genes, retrotransposons

Abstract

Aegilops tauschii (Coss.) Schmal. ($2n = 2x = 14$, DD) (syn. *A. squarrosa* L.; *Triticum tauschii*) is well known as the D-genome donor of bread wheat (*T. aestivum*, $2n = 6x = 42$, AABBDD). Because of conserved synteny, a high-density map of the *A. tauschii* genome will be useful for breeding and genetics within the tribe Triticeae which besides bread wheat also includes barley and rye. We have placed 249 new loci onto a high-density integrated cytological and genetic map of *A. tauschii* for a total of 732 loci making it one of the most extensive maps produced to date for the Triticeae species. Of the mapped loci, 160 are defense-related genes. The retrotransposon marker system recently developed for cultivated barley (*Hordeum vulgare* L.) was successfully applied to *A. tauschii* with the placement of 80 retrotransposon loci onto the map. A total of 50 microsatellite and ISSR loci were also added. Most of the retrotransposon loci, resistance (R), and defense-response (DR) genes are organized into clusters: retrotransposon clusters in the pericentromeric regions, R and DR gene clusters in distal/telomeric regions. Markers are non-randomly distributed with low density in the pericentromeric regions and marker clusters in the distal regions. A significant correlation between the physical density of markers (number of markers mapped to the chromosome segment/physical length of the same segment in μm) and recombination rate (genetic length of a chromosome segment/physical length of the same segment in μm) was demonstrated. Discrete regions of negative or positive interference (an excess or deficiency of crossovers in adjacent intervals relative to the expected rates on the assumption of no interference) was observed in most of the chromosomes. Surprisingly, pericentromeric regions showed negative interference. Islands with negative, positive and/or no interference were present in interstitial and distal regions. Most of the positive interference was restricted to the long arms. The model of chromosome structure and function in cereals with large genomes that emerges from these studies is discussed.

Introduction

The D-genome is the least polymorphic, and consequently most difficult to map, among the three genomes (A, B and D) of bread wheat (*Triticum aestivum* L.) (Kam-Morgan *et al.*, 1989; Röder *et al.*, 1998). However, the diploid D-genome donor species *A. tauschii* Coss. is highly polymorphic and shares al-

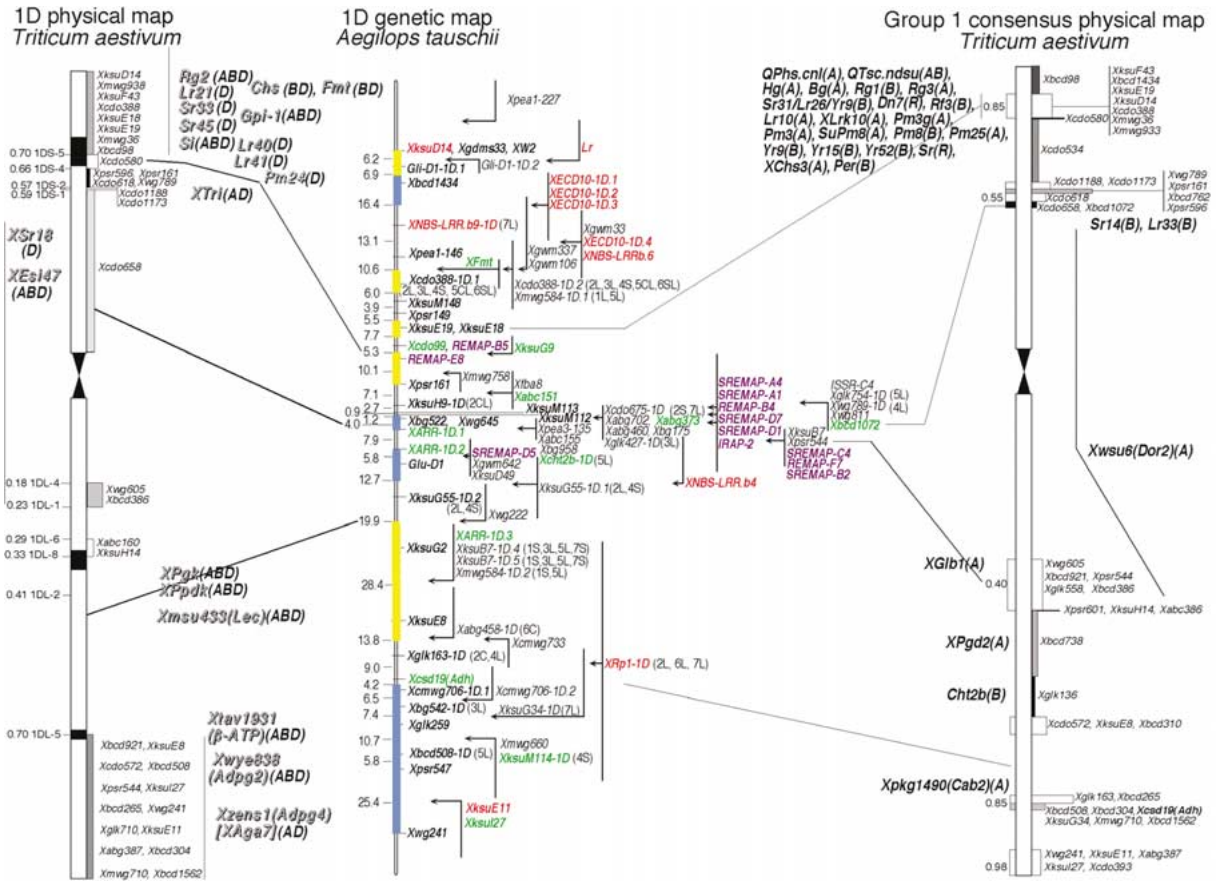

Figure 1. Genetic linkage maps of chromosomes 1D to 7D of *Aegilops tauschii*. Loci of the basic map, ordered at LOD >2.0, are indicated in bold. Vertical lines join groups of the markers mapping at LOD <2.0 at their probable locations. Arrows indicate the most probable location of these groups. Lines to the left of the *A. tauschii* chromosome map connect similar segments on the *Triticum aestivum* physical and *A. tauschii* genetic maps. Lines on the right connect some common loci between the physical and genetic maps. Yellow bars denote areas with negative interference, blue with positive, and the remaining areas indicate no interference. Red and green letters indicate resistance and defense-response genes, and purple-colored letters indicate retrotransposon markers. Agronomically important genes, genes that encode proteins, and morphological markers mapped in the Triticeae by other authors are shown in outlined letters for the D-genome and in bold letters for the other genomes. Markers that have different locations on the genetic vs. the physical map are boxed.

most complete homology to the D-genome of bread wheat. It thus provides an excellent resource for genetic mapping of wheat (Kam-Morgan *et al.*, 1989; Gill *et al.*, 1991b) as well as barley (*Hordeum vulgare* L.), rye (*Secale cereale* L.) and other Triticeae species. It also has a lower DNA content (4024 Mb) than *A. speltoides*, the B-genome donor (4886 Mb), and *T. monococcum*, the A-genome donor (5751 Mb) (Arumuganathan and Earle, 1991; Bennett and Leitch, 1995).

A high-density map sampling all classes of markers and different components of the genome will be most useful. Our previous map (Gill *et al.*, 1991b; Boyko *et al.*, 1999) was based mainly on genomic sequences of undermethylated DNA (a *Pst*I-digested library), cDNAs, AFLPs, and a few known gene loci. In the current map, we include retrotransposon markers (Flavell *et al.*, 1998; Kalendar *et al.*, 1999; Waugh *et al.*, 1997) to sample the underlying retrotransposon populations that constitute the major portion of the repetitive fraction of the genome. Retrotransposons are propagated by a cycle of transcription, reverse transcription, and integration (Kumar and Bennetzen, 1999). Each insertional event creates a link between the well-conserved long terminal repeats (LTRs) of the retrotransposon and the flanking DNA of the genome. Retrotransposon marker systems exploit the conservation of the LTRs in the design of PCR primers to detect retrotransposon insertion sites. The inter-retrotransposon amplified polymorphism (IRAP)

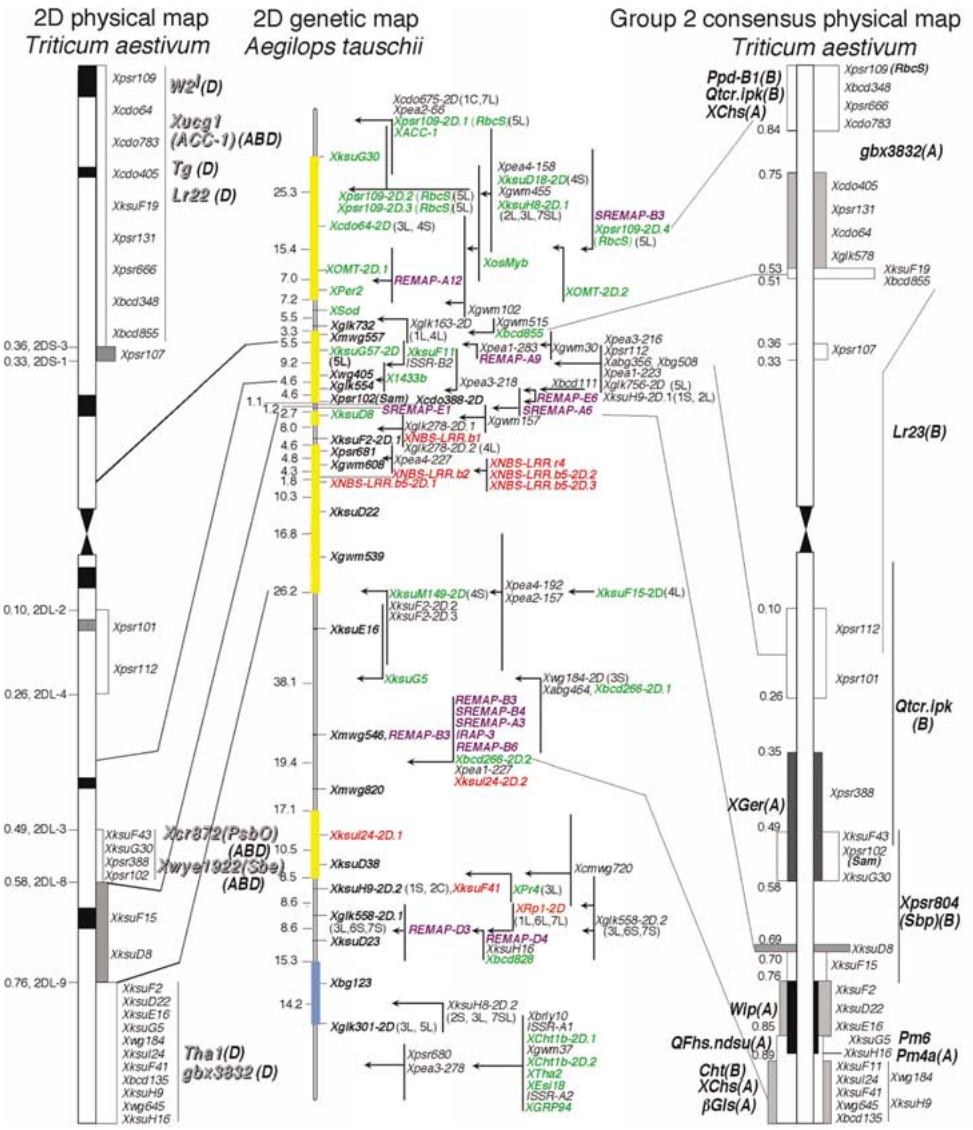

Figure 1. Continued.

and retrotransposon-microsatellite amplified polymorphism (REMAP) methods rely on PCR amplification between nearby LTRs and between LTRs and nearby microsatellites, respectively.

Within the Triticeae, the BARE-1 retrotransposon of barley is present in more than 10^4 copies (Vicient *et al.*, 1999) and is active transcriptionally (Suoniemi *et al.*, 1996b) and translationally (Jääskeläinen *et al.*, 1999). *BARE*-1 plays a major role in genome dynamics in the genus *Hordeum* as a whole (Vicient *et al.*, 1999) and has proven useful in distinguishing barley varieties and even individuals within wild barley populations (Kalendar *et al.*, 2000). Elements very similar to *BARE*-1 are also present in wheat (Matsuoka and Tsunewaki, 1996) and rye (Pearce *et al.*, 1997).

Mapping of markers related to resistance gene analogues (RGA) and defense-response (DR) or pathogenesis-related (PR) genes (Bryngelsson *et al.*, 1994; Collins *et al.*, 1998; Seah *et al.*, 1998; for review, see Muthukrishnan *et al.*, 2001) is important for map-based cloning, marker-assisted selection, and candidate gene analysis of the qualitative and quantitative disease resistance loci (Li *et al.*, 1999; Faris *et al.*, 1999; Seah *et al.*, 2000).

We present an integrated high-density genetic linkage map of *A. tauschii* consisting of retrotransposon,

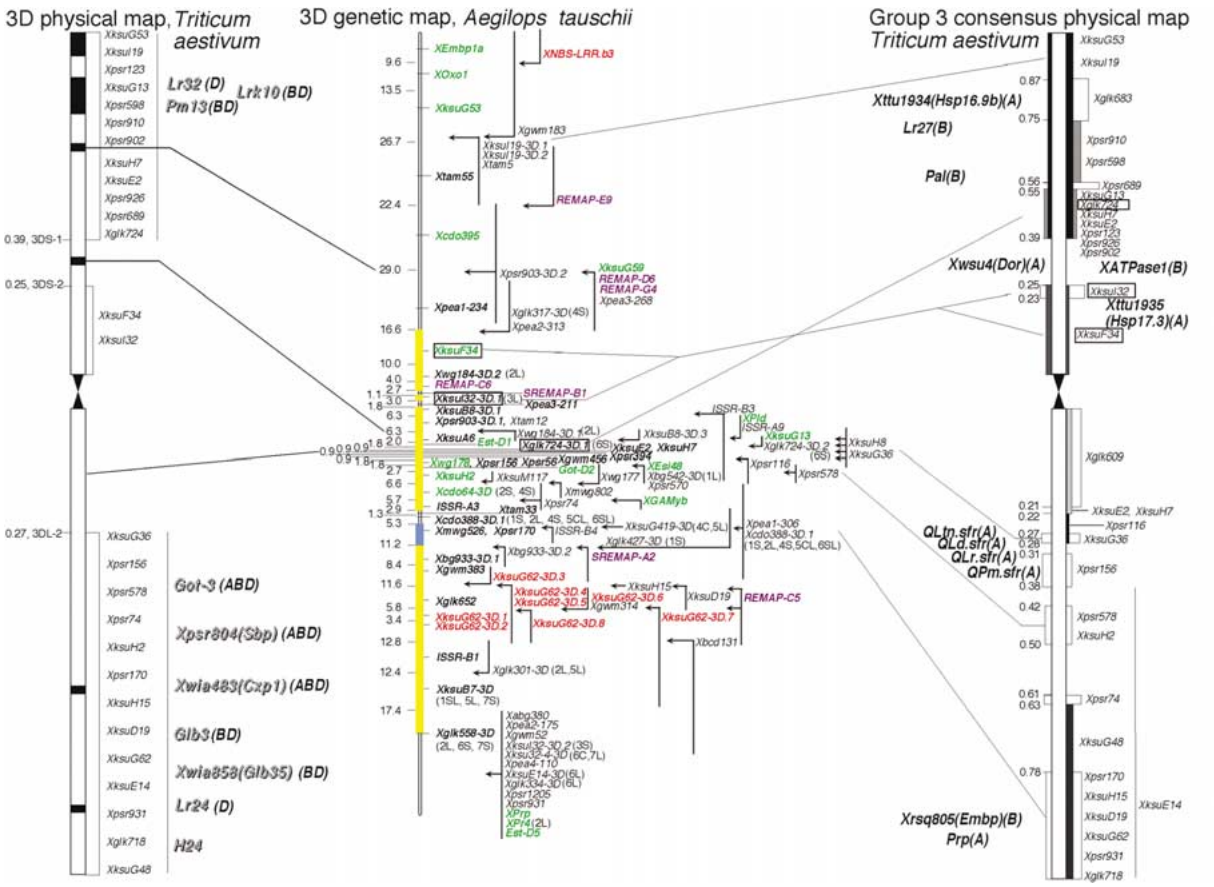

Figure 1. Continued.

RGA, DR, and microsatellite (MS) markers incorporated into the previously published map (Boyko *et al.*, 1999). We also present an analysis of the *A. tauschii* genetic and *T. aestivum* D-genome physical mapping data to explore cereal chromosome structure and function for theoretical and applied molecular genetic applications.

Materials and methods

Plant materials

A population of 56 F_2 plants and F_3 families representing individual F_2 plants from an *A. tauschii* var. *meyeri* (TA1691) × var. *typica* (TA1704) cross was used (Gill *et al.*, 1991b). All plant material is maintained by the Wheat Genetics Resource Center (WGRC), Kansas State University, Manhattan, KS.

Marker resources

A total of 118 clones of resistance gene analogues and defense-response genes from collections maintained by the WGRC and the KSU Plant Pathology Department were used for RFLP analysis. All procedures for RFLP analysis were previously described in Gill *et al.* (1991b) and Boyko *et al.* (1999). Segregation data for six defense-related genes and some protein and wheat microsatellite markers were provided by L. Huang (*Lr, XksuD14, Xgdms33, XW2*, and *Gli-D1*) and W.L. Li (α-phospholipase, chitinase 2 and chalcone isomerase (*XChi-Dra*I)), Kansas State University, and J. Faris (acetyl-CoA carboxylase), North Dakota State University, Fargo, ND.

Fifty primer pairs of wheat microsatellites (WMS) representing all chromosomes of the D genome of hexaploid wheat were chosen for mapping. The WMS designation, primer sequences, fragment size in 'Chinese Spring' (CS), chromosome location of the amplified loci, and annealing temperature for PCR and

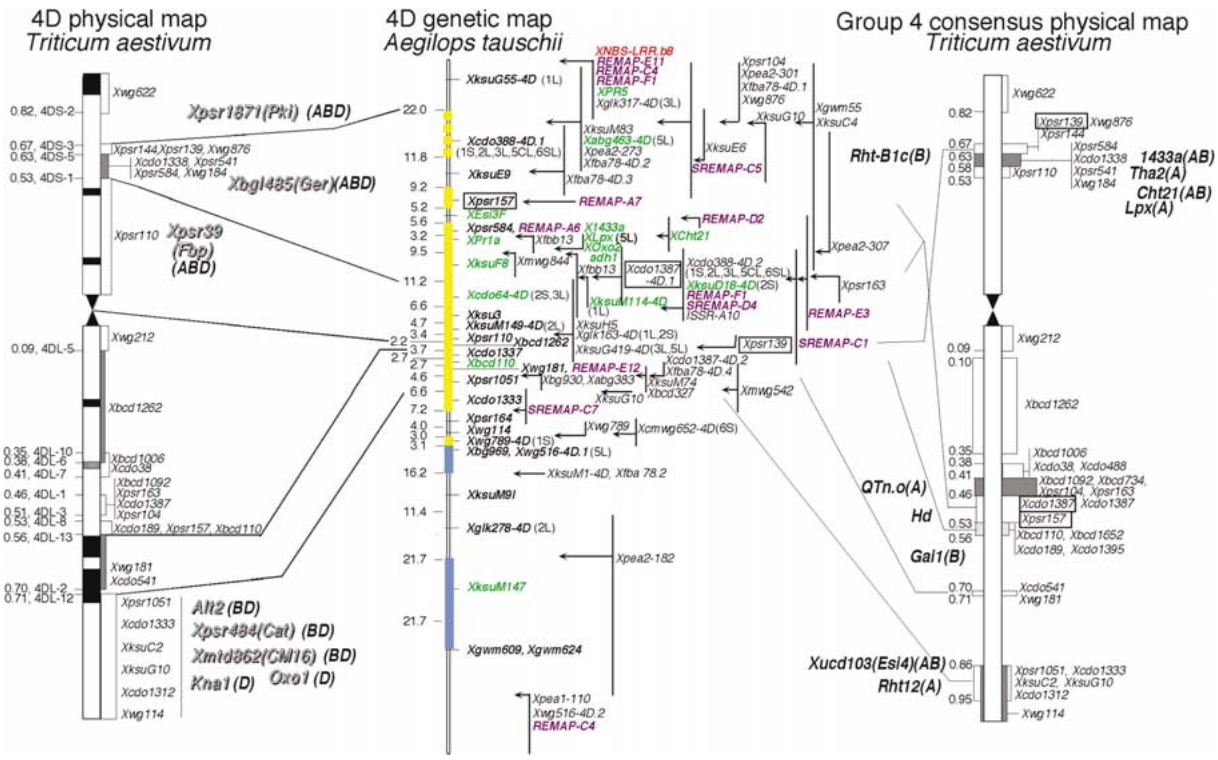

Figure 1. Continued.

fragment detection have been previously described (Plaschke *et al.*, 1996; Röder *et al.*, 1995, 1998).

For retrotransposon-based markers, IRAP (inter-retrotransposon amplified polymorphism) employs primers matching the LTRs of retrotransposons oriented away from the LTRs themselves. The REMAP and SREMAP (retrotransposon-microsatellite amplified polymorphism) method utilizes IRAP-type LTR primers in combination with simple-sequence repeat (SSR) or microsatellite primers anchored by a selective base at their 3′ end. The ISSR (inter-simple-sequence-repeat) method employs SSR primers similar to those used in REMAP, but with the absence of the LTR primer. The ISSR, REMAP, and IRAP primers and their combinations used in this study are listed in Table 1. The LTR primer sequences and PCR amplification procedures have been previously described (Kalendar *et al.*, 1999, 2000). Information on mapped loci is provided in Tables 2 and 3.

Sequence analysis

The construction of the *Pst*I genomic library of *A. tauschii* has been previously described (Gill *et al.*, 1991b). *Escherichia coli* cultures containing plasmids were grown in 1 ml of Terrific Broth (Sigma-Aldrich) containing 100 mg/l of ampicillin for 20 h at 250 rpm and 37 °C. Plasmids were isolated from colonies with a Qiagen Biorobot 3000 and Turbo 96 (Qiagen, Valencia, CA) isolation kits. Templates were 5′ single-pass-sequenced using M13 forward (IDT, Coralville, IA) primers and the BigDye terminator kit version 1 (Applied Biosystems, Foster City, CA). Sequence reactions were precipitated with 60% v/v final concentration of isopropanol and washed with 70% v/v ethanol. After being air-dried, the pellets were resuspended in highly de-ionized formamide (Applied Biosystems). Sequence analysis was performed on an ABI 3700 DNA Analyzer (Applied Biosystems). Sequencing data were analyzed for quality and vector sequence removed using Phred and Cross-match (Ewing *et al.*, 1998; Ewing and Green, 1998; Gordon *et al.*, 1998). Sequences were aligned to public databases using BLASTX.

Linkage and statistical analysis

Linkage analysis was performed as previously described by Boyko *et al.* (1999). The cytogenetic maps were constructed using markers common to the

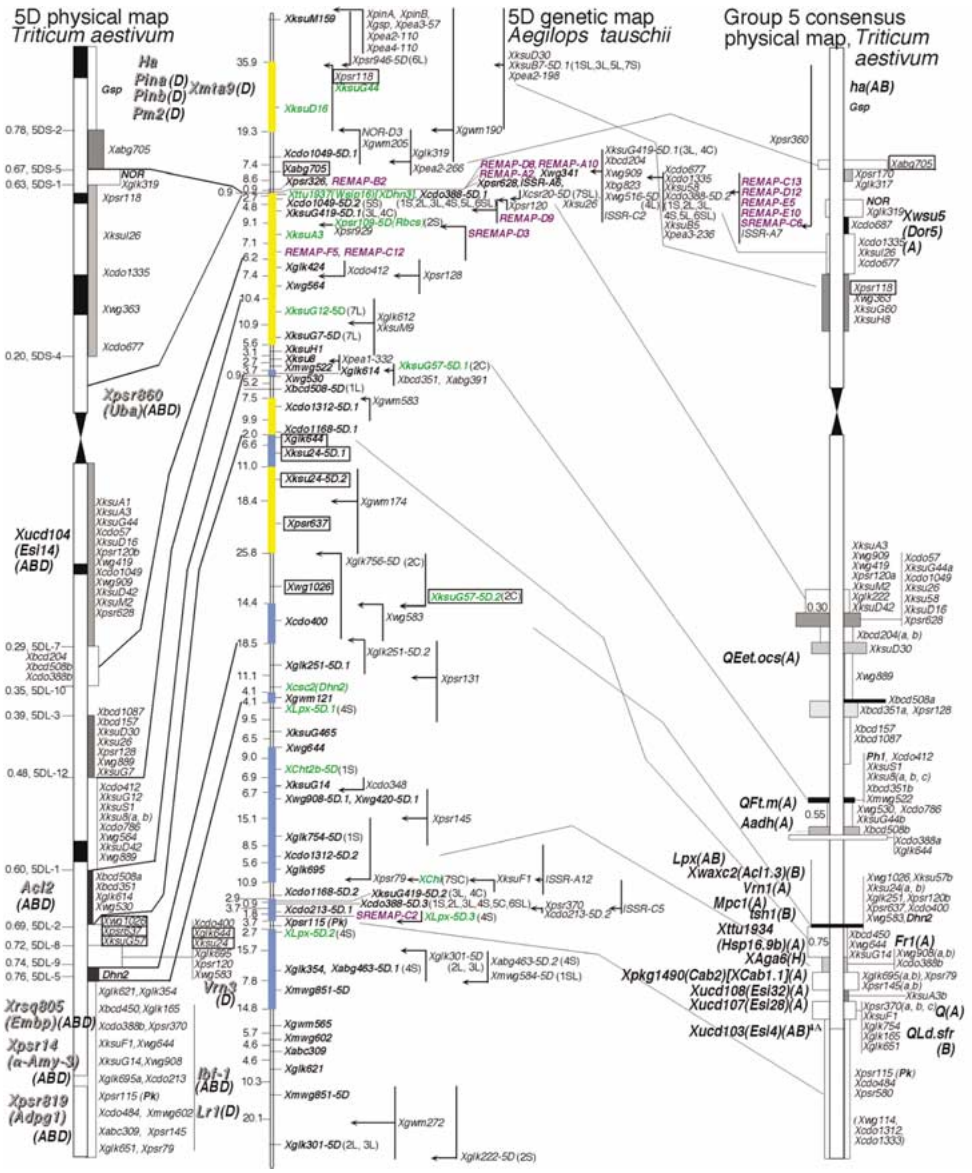

Figure 1. Continued.

A. tauschii genetic (WGRC home page, Figure 1) and *T. aestivum* physical maps (Gill *et al.*, 1993, 1996a, b; Hohmann *et al.*, 1994; Delaney *et al.*, 1995a, b; Mickelson-Young *et al.*, 1995; Weng *et al.* 2000) of the seven D-genome chromosomes. Data on the size of wheat D-genome chromosomes and their segments were taken from Gill *et al.* (1991a) and Endo and Gill (1996). We analyzed the relationship between the genetic and physical size of chromosomes, and recombination rate and physical density of markers in different chromosome segments classified as: *telomeric or subtelomeric* (near the end of a chromosome arm), *distal* (in the distal third of a chromosome arm), *proximal* (*pericentromeric*) (in the third of a chromosome arm on either side of the centromere), or *interstitial* (in the third of the chromosome arm between the distal and proximal regions).

All of the calculations were done with the complete *A. tauschii* maps where uncertain markers (markers that are ordered at LOD <2.00) are placed in their most likely locations on the basic map (LOD >2.00) by inserting them among the markers using the com-

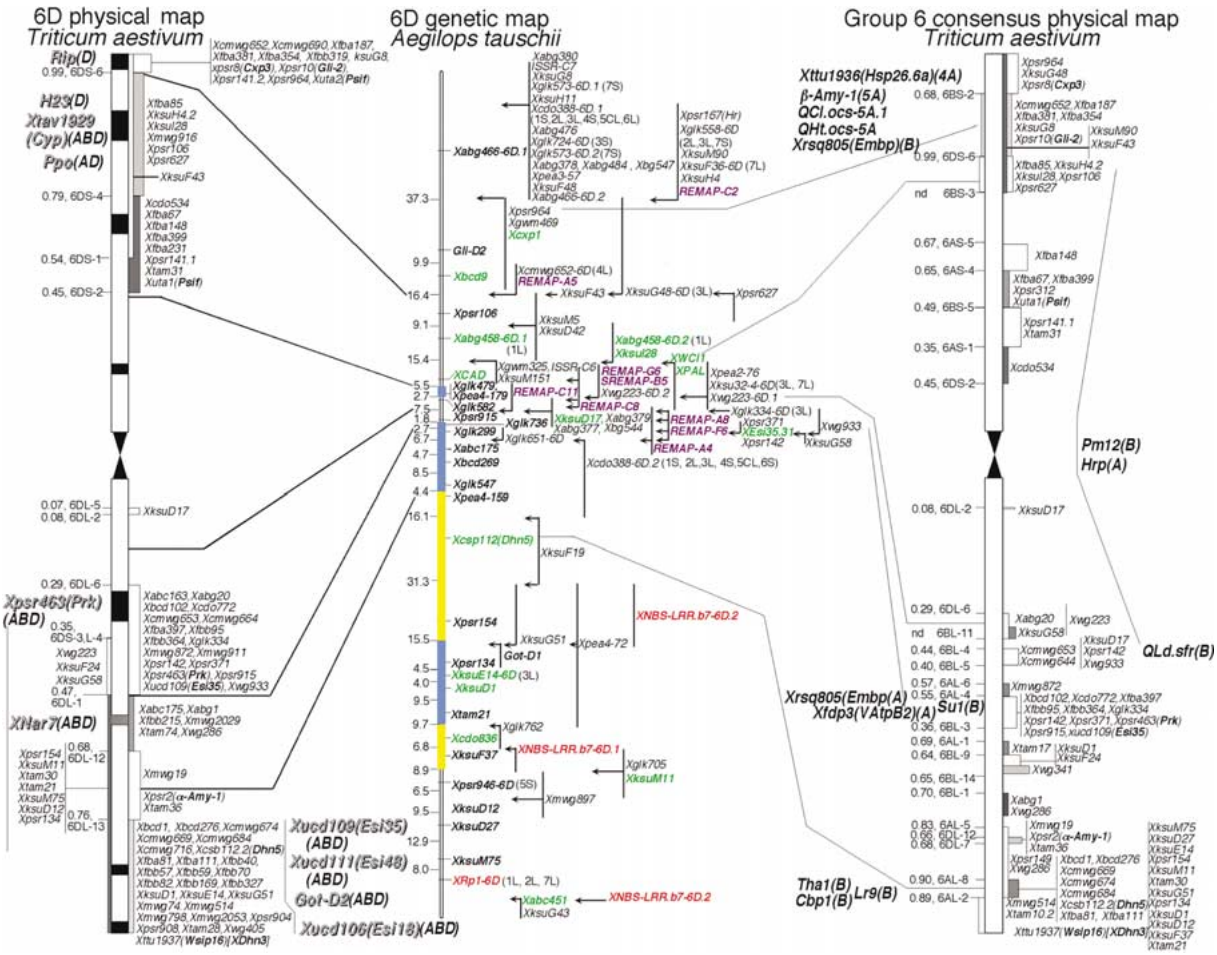

Figure 1. Continued.

mand TRY of the MAPMAKER 2.0 program (Lander *et al.*, 1987). If more than one marker were placed in an interval, they were arranged in the most likely order using the command COMPARE. We think that use of complete maps is reasonable, because it allows for the maximum amount of information per map. In support of this approach, results of the same type of calculations performed on 1D basic maps at LOD = 2.00 and LOD = 3.00 showed the same trends that were revealed using the complete map. Complete *A. tauschii* maps are not presented in this paper but are available on the Internet (WGRC home page, Figure 1).

The test for positive/negative/no interference was based on the basic map data. The following hypotheses were tested.

Hypothesis 1. Recombination rate is uniform along the physical chromosome length. We define the recombination rate of a whole chromosome or its segment as the number of cM per μm. We first calculated the observed recombination rate (R_i) for each interval as $R_i = \mathrm{cM}_i / S_i$, where cM_i is the observed cM length of the ith interval, and S_i is the physical length of an interval/segment in μm. We then calculated an expected recombination rate $R_j = \mathrm{cM}_j / L_j$, where cM_j is the observed genetic length of the jth chromosome and L_j is the observed physical length of a jth chromosome in μm. A goodness-of-fit (GOF) (McClave and Dietrich, 1982) test of observed vs. expected recombination rate was performed. Although the GOF test is applied to count data, it is justifiable here because cMs are counts of recombination events in a population.

Hypothesis 2. The genetic lengths of the seven A. tauschii *chromosomes are not different.* We performed the GOF test of genetic length of each chromosome vs. expected genetic length. Expected genetic length was calculated by dividing the total genetic

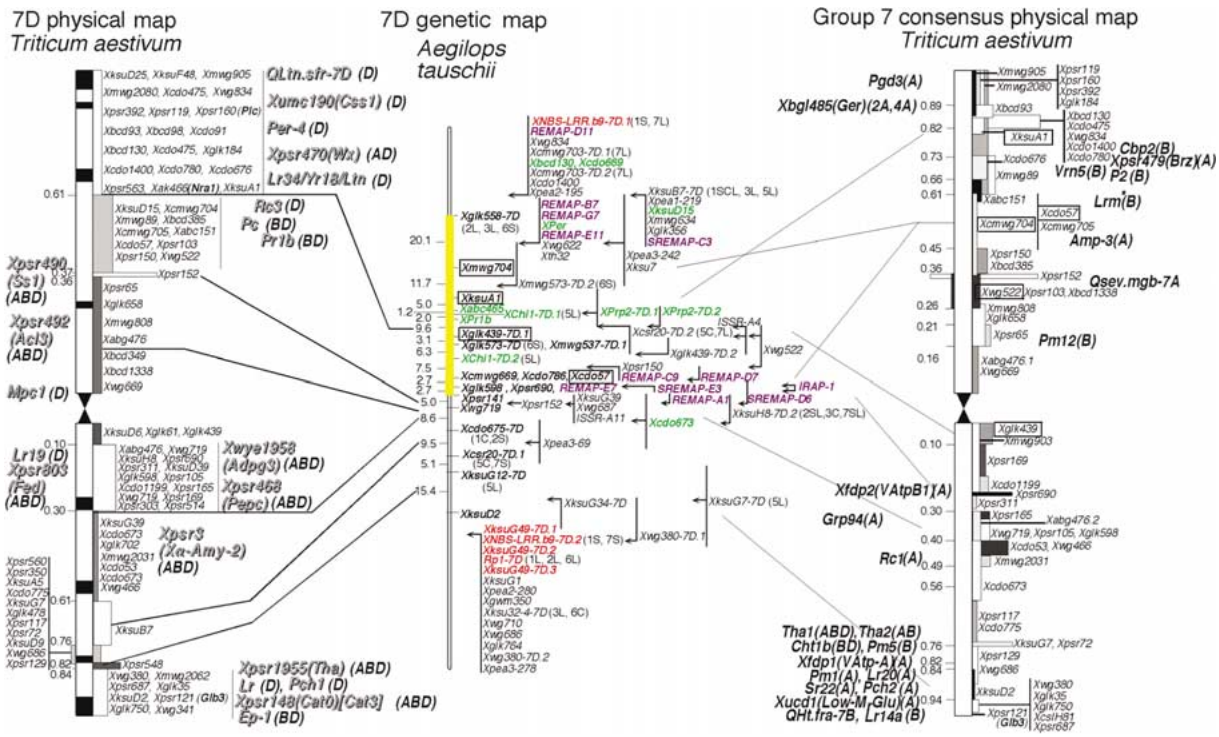

Figure 1. Continued.

length of the *A. tauschii* genetic map by the number of chromosomes.

Hypothesis 3. The marker density is uniform along the physical chromosome length. We calculated the physical density of markers (number of markers per μm) in different chromosome intervals/segments. Because the number of markers mapped genetically or physically may vary for each chromosome, we used a coefficient to standardize the number of markers on each chromosome map and to adjust the number of markers mapped in each interval. In this way it was possible to compare the physical density of markers on genetic and physical maps. It was also possible to compare the physical density of markers in different segments of each chromosome or over the whole genome. The coefficient was calculated as $k_j = M_5/M_j$, where M_5 is the number of markers on the chromosome 5D genetic map (the highest number of markers mapped in *A. tauschii* chromosomes) and M_j is the number of markers on the genetic or physical map of the jth chromosome. The standardized physical density of markers in each chromosome segment was calculated as follows. The calculated observed physical density of markers is $\mathrm{PD}_i = k_j \times M_i/S_i$, where M_i is the number of markers in the ith segment, and S_i is the physical size of the same segment in μm. The calculated expected physical density of markers is $\mathrm{PD}_{ej} = k_j \times M_j/L_j$, where M_j is the number of markers on the genetic map of the jth chromosome, and L_j is the physical length of the jth chromosome in μm. The calculated expected physical density of markers for all chromosomes is $\mathrm{PD}_e = 7 \times M_5/L$, where M_5 is the number of markers on a chromosome 5D genetic map, and L is the total physical length of all D-genome chromosomes in μm. A GOF test for observed vs. expected physical density, and for observed physical density based on genetic map data vs. that based on physical map data, was performed.

Hypothesis 4. Recombination rate and physical density of markers are correlated. The correlation between recombination rate and physical density of markers was calculated using the 'Spearman's rank correlation coefficient' formula (McClave and Dietrich, 1982).

Hypothesis 5. There is no positive or negative crossover interference in the genetic map of the TA1691 × TA1704 hybrid. Maximum-likelihood (ML) estimates of coefficient of coincidence (c) (Peng *et al.*, 2000) were made to detect positive or negative crossover interference.

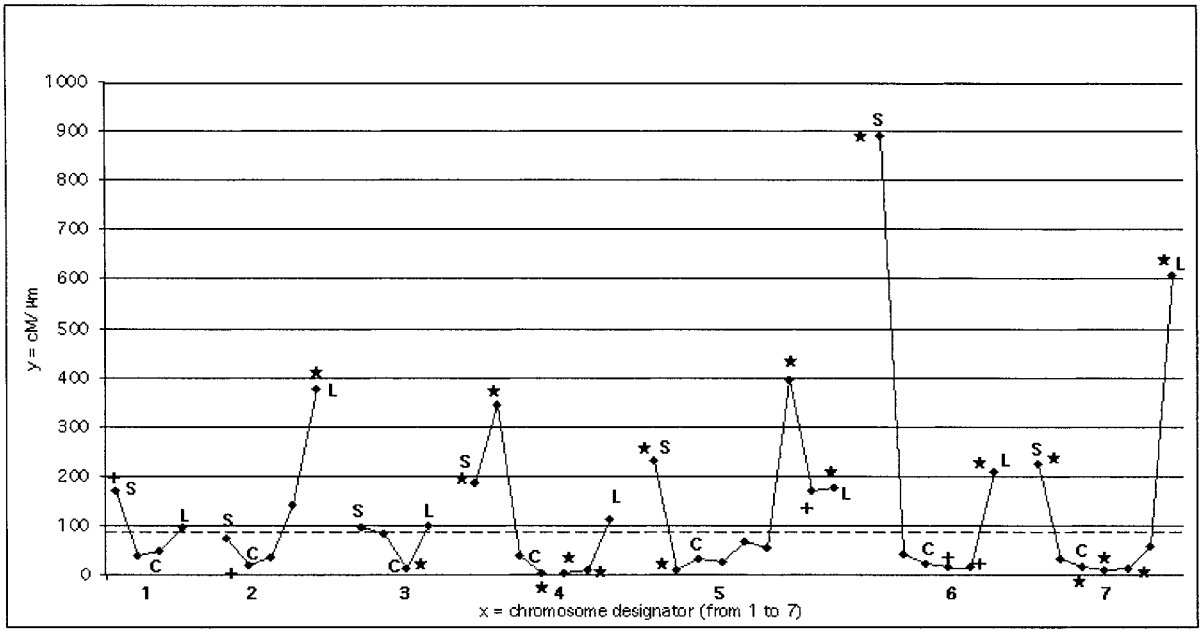

Figure 2. Recombination rate (cM/μm) in segments of *Aegilops tauschii* chromosomes. The dashed line indicates expected cM/μm in case of inter-chromosomal comparison. + and * indicate cM/μm different from the expected rate at $\alpha = 0.025$ and $\alpha = 0.005$, respectively. S, short arm; L, long arm; C, pericentromeric region.

Results

Sequencing results of ksu *RFLP library*

The genomic library constructed by Gill *et al.* (1991b) contained 223 low-copy clones of inserts from a *Pst*I digest of genomic DNA. *Pst*I cuts only non-methylated DNA and thus enriches for transcribed regions of DNA. These clones were used as RFLP markers and make up the *ksu* RFLP library. Only 141 of the clones were polymorphic (Gill *et al.*, 1991b). Of the 223 clones, 209 were 'single-pass'-sequenced. To determine whether the library clones contained open reading frames, the sequences were compared to those of protein databases with BLASTX, which translates the DNA sequence in all six reading frames. Thirty-one had strong alignments to unknown or hypothetical proteins. Of the 209 clones, 77 were found to align to genes of known function, meaning that the clones had predicted open reading frames and high sequence similarity to proteins of known function. Of these, *ksuD14, ksuE11, ksuF43, ksuF64, ksuF46, ksuG49, ksuG62, ksuI12, ksuI15*, and *ksuI24* contain sequences similar to those of cloned resistance genes. Four clones, *ksuD28, ksuD31, ksuF40*, and *ksuM11*, are similar to defense-response genes. *KsuM147* is classified as a stress response gene, while *ksuD1, ksuD13, ksuD15, ksuD21, ksuD24, ksuE13, ksuE17, ksuE11*, and *ksuH40* are homologous to genes involved in plant defense signal transduction. Mobile element sequences were found in clones *ksuD4, ksuF71*, and *ksuG44*. R-genes and defense-related *ksu* clones, as well as other mapped clones related to defense genes in the public database, are highlighted on the maps (Figure 1).

Individual chromosome maps

Chromosome 1D

The map (Figure 1) contains 97 loci, including 24 defense-related loci and 21 PCR-based markers (Tables 2, 3, and 4). The most distinguishing feature of the 1D map (see top of 1D and group 1 consensus physical maps) is the cluster of agronomically useful genes in the telomeric end of its short arm including resistance genes for leaf rust (*Lr21, Lr40*, and *Lr41*), stem rust (Sr33 and Sr45) and powdery mildew (*Pm24*). Other defense-related loci located on homoeologous chromosomes 1A and 1B are shown on the group 1 consensus map (see also Sandhu *et al.*, 2001). Significantly, four loci for the extra-cellular domain of a receptor-like kinase (*XECD10*), two RGA loci (*NBS-LRR*) and a DR locus (*XFmt*, flavonol-7-*O*-methyl transferase) form a cluster of resistance genes in the

Table 1. Primers used for ISSR, REMAP, and IRAP mapping. Primers were designed to match the 5′ LTR of the BARE-1a sequence (accession Z17327, base 309-2137). The reverse primer (7286) 5′-GGA ATT CAT AGC ATG GAT AAT AAA CGA TTA TC-3′ is complementary to 369-391; primer (9900) 5′-GAT AGG GTC GCA TCT TGG GCG TGA C-3′ is complementary to 10662-10685.

Name	Primers		Number of markers
REMAP-A	$(GA)_9C$	7286	12
REMAP-B	$(CT)_9G$	7286	7
REMAP-C	$(AC)_9G$	7286	13
REMAP-D	$(AG)_9C$	7286	14
REMAP-E	$(AC)_9C$	7286	12
REMAP-F	$(TG)_9A$	7286	7
REMAP-G	$(CAC)_7T$	7286	7
SREMAP-A	$(GCT)_6A$	9900	5
SREMAP-A	$(CTC)_6A$	9900	5
SREMAP-A	$(AGC)_6G$	9900	7
SREMAP-A	$(ACC)_6G$	9900	8
SREMAP-A	$(AGC)_6A$	9900	3
ISSR-A	$(ACC)_6G$		11
ISSR-B	$(AGC)_6C$		5
ISSR-C	$(AGC)_6G$		7
IRAP		9900	3
TOTAL			126

same region of the 1D genetic map. The most distal 1DS frame map locus *XksuD14* is also an RGA and is tightly linked to *Lr40/Lr21* genes (Li and Gill, 2001). The pericentromeric region of 1D is characterized by suppressed recombination and most of the retrotransposon loci are clustered in this region. Chitinase 2 (*XCht22*), and a family of aldose reductase-related loci (*XARR*) are clustered in the proximal region of the long arm. One of the family members of maize rust gene Rp1 (Collins *et al.*, 1998) maps to the 1DL distal region as well as to the long arms of chromosomes 2D, 4D, 6D, and 7D. Other RGA and DR loci are dispersed along the length of the chromosome.

Chromosome 2D

The map of chromosome 2D consists of 115 loci (Figure 1, Tables 2, 3, and 4). Of these, 41, roughly 1/3 of the loci on 2D, are defense-related, the most among all chromosomes. There are 36 PCR-based markers including AFLP, microsatellite, ISSR, and retrotransposon markers. Practically all of the loci distal to 50% on the short arm are defense-related including a transcription activation domain locus (*XOsMyb*), two *O*-methyltransferase loci (*XOMT*), a peroxidase locus (*XPer2*), and a superoxide dismutase locus (*XSod*). The non-defense-related loci include a REMAP, a SREMAP, two microsatellite loci (*gwm102, gwm455*) and a few others of unknown function. Two clusters of defense genes are present in the 2DL arm; an NBS-LRR cluster of six loci in the distal region, and a cluster of DR loci including thaumatin (*XTha2*), endoplasmic reticulum heat shock protein (*XGRP94*), an early salt stress response gene (*Esi18*), and two chitinase (*XCht1b*) loci at the telomeric end. Clusters of retransposon-related loci are present in the interstitial and distal regions of 2DL.

Chromosome 3D

The map for chromosome 3D consists of 105 loci (Figure 1, Tables 2, 3 and 4), including 23 PCR-based markers. There are 27 defense-related loci; three each are found at the telomeric ends of both arms, three in the interstitial region of short arm, three in the pericentromeric region, and a cluster of six in the interstitial region of the long arm. A cluster of eight NBS-LRR family members is found in the distal region of 3DL.

Chromosome 4D

A total of 92 loci were mapped onto chromosome 4D (Figure 1), including 16 defense-related loci and 12 retrotransposons, and ten other PCR-based markers (see Tables 2, 3, and 4). A prominent feature of the 4D map is that marker-rich regions are located in the interstitial regions of both arms. The 4DS interstitial marker-rich region is further notable for a cluster of defense-response genes including chitinase 2 (*XCht21*), a Pr1a homologue (*XPr1a*), a 14-3-3 protein (*X1433a*), lipoxygenase (*XLpx*), an early salt stress response gene (*XEsi33F*), and oxalate oxidase (*XOxo2*). Interestingly, retrotransposon-related loci map in the relatively marker-poor telomeric ends including an RGA locus and a DR locus in the 4DS telomeric region.

Chromosome 5D

In all, 137 loci were placed on chromosome 5D (Figure 1, Tables 2, 3, and 4). Fourteen defense-response loci, including three for lipoxygenase (*XLpx*), a chitinase 2 gene (*XCht2b*), chalcone isomerase (*XChi*), and a dehydrin (*XDhn2*) locus mapped to the distal region of the long arm. They are not tightly clustered, being

Table 2. Number of loci mapped in each of seven (1D to 7D) *Aegilops tauschii* chromosomes.

Chromosome	Loci in the map		Basic map (No. of loci)		Defense-related loci	AFLP	Micro-satellite	ISSR	REMAP & SREMAP	IRAP
	1	2	1	2	2	1	2	2	2	2
1D	68	97	25	37	24	3	5	1	11	1
2D	76	115	21	32	41	11	8	3	14	1
3D	87	105	28	40	27	6	5	5	7	0
4D	54	92	17	30	16	6	3	1	14	0
5D	107	137	46	66	14	7	7	5	14	0
6D	83	103	26	29	20	5	2	2	9	0
7D	72	83	13	22	18	6	1	2	11	1
Total	547	732	176	256	160	44	31	19	80	3

1 – Boyko *et al.* (1999)
2 – present study

interspersed with RFLP, WMS, ISSR, and REMAP markers. Eleven REMAP markers comprising two major clusters and a few isolated loci were found in the pericentromeric region.

Chromosome 6D

The map for chromosome 6D was assembled from 103 loci, including 20 defense-related genes, nine retrotransposon, and nine other PCR-based markers (Figure 1, Tables 2, 3, and 4). A cluster containing drought- and/or salt stress-associated protein (*XWCI1*), phenylalanine ammonia-lyase (*XPal*), cinnamyl alcohol dehydrogenase (*XCAD*) and three other DR loci is located in the interstitial region of 6DS. A cluster of REMAP loci is located in the pericentromeric region. A locus for an early salt-stress response gene (*XEsi35.31*) is located in the interstitial region of the long arm. The *XNBS-LRR.b7-6D.2, XRp1-6D* loci at the telomeric end; *XNBS-LRR.b7-6D.1* and a dehydrin locus (*Xcsp112*) are located in the distal region of the long arm.

Chromosome 7D

For chromosome 7D, a total of 83 loci were placed on the map, including 18 defense-related loci, 12 retrotransposon markers, and nine other PCR-based markers (Figure 1, Tables 2, 3 and 4). Clusters of retrotransposon-related loci were located in the distal region of 7DS and the pericentromeric region. A cluster composed of loci for chalcone isomerase (*XChi-7D.1*), two proline-rich proteins (*XPrp2-7D.1* and *XPrp2-7D.2*) and *XPr1b* mapped to the interstitial region of 7DS. Another chalcone isomerase (*XChi-7D.2*) locus was found in the pericentromeric region. A cluster of R-gene loci related to Rp1 gene is located in the telomeric region of the long arm.

Recombination rates across the A. tauschii *genome*

We found no correlation between the number of markers and the genetic length for each of the seven chromosome maps (unpublished results). Hence, we did not standardize recombination rate values in order to compare them among different chromosomes. Results for all seven *A. tauschii* chromosome segments (Figure 2; see also WGRC home page, Figures 2, 4, 6, 8, 10, 12, and 14) disagree with hypothesis 1 (see Materials and methods) and suggest that each chromosome has a unique pattern of recombination rate. In general, recombination is strongly suppressed in the pericentromeric regions of chromosomes and is high in the telomeric regions. The distinctive recombination patterns of individual chromosomes can be described as follows.

Chromosomes 5D, 6D, and 7D have significantly high rates of recombination at both telomeric ends. Chromosome 6D is unique in having the highest rate of recombination in the 6DS telomeric region, among all short or long arm telomeric ends. The 50% of the long arm of 6D has significant suppression of recombination. Chromosome 7D long arm telomeric region has the highest rate of recombination among all long arm telomeric regions. Recombination is suppressed in most of 7D excluding the distal regions of both arms. The regions of strong suppression of recombination are adjacent to the terminal regions of 6DS and 7DL with extremely high rates of recombination. The third highest rate of recombination is

Table 3. Chromosome locations of resistance and defence response genes, mapped in *Aegilops tauschii* in this study.

Gene and/or product	Symbol of the locus	No. of loci	Clone designator	Enzyme for DNA digest	No. of scored bands/total no.	Source of the clone	Supplier
1D short arm							
Extracellular domain of Lr10	*ECD10*	4	ECD10	EcoRV&XbaI	2/6&2/4	wheat	B. Keller
NBS-LRR	*NBS-LRR.b9* (7L)	1	b9	EcoRV	6/8	barley	P. Schulze-Lefert
NBS-LRR	*NBS-LRR.b6*	1	b6	XbaI	2/3	barley	P. Schulze-Lefert
Flavonoid 7-*O*-methyl transferase	*Fmt*	1	pBH72-F1	DraI	1/8	barley	D. Collinge
1D long arm							
Chitinase 2b	*Cht2b* (5L)	1	pBH72-N12	BamHI	1/10	barley	D. Collinge
Aldose reductase related	*ARR*	3	pg2269	XbaI	3/3	barley	F. Salamini
NBS-LRR	*NBS-LRR.b4*	1	b4	HindIII	1/5	barley	P. Schulze-Lefert
NBS-LRR	*Rp1* (2L,6L,7L)	1	Rp1	EcoRI	4/9	maize	S. Hulbert
2D short arm							
Transcription activation domain	*osMyb*	1	BSMyB4B	HindIII	1/11	rice	I. Coraggio
O-methyltransferase	*OMT*	2	OMT	HindIII	4/9	maize	P. Puigdomenech
Peroxidase	*Per2*	1	POX22.3	EcoRI	2/6	rice	F. White
Superoxide dismutase	*Sod*	1	CSU182	XbaI	1/1	maize	T. Masket
2D long arm							
14-3-3 protein ion channel regulator	*1433b*	1	pHv1433b	DraI	1/3	barley	D. Collinge
NBS-LRR	*NBS-LRR.b1*	1	b1	DraI	1/3	barley	P. Schulze-Lefert
NBS-LRR	*NBS-LRR.b2*	1	b2	EcoRI	2/3	barley	P. Schulze-Lefert
NBS-LRR	*NBS-LRR.r4*	1	r4	EcoRI	2/2	rice	P. Schulze-Lefert
NBS-LRR	*NBS-LRR.b5*	3	b5	EcoRI	4/5	barley	P. Schulze-Lefert
Pr4	*Pr4* (3L)	1	pBH72-B8	BamHI	2/8	barley	D. Collinge
NBS-LRR	*Rp1* (1L,6L,7L)	1	Rp1	EcoRI	4/9	maize	S. Hulbert
Chitinase	*Cht1b*	2	Barchi3	XbaI	1/8	barley	S. Muthukrishnan
Thaumatin	*Tha2*	1	pBH72-C6	XbaI	1/2	barley	D. Collinge
Early-salt-induced protein	*Esi18*	1	Esi18	BamHI	1/4	*Lophopyrum elongatum*	P. Gulick
Endoplasmic heat shock protein, 'endoplasmin'	*GRP94*	1	HVGRP94HO (pBH6-601)	EcoRV	1/1	barley	D. Collinge
3D short arm							
DNA-binding protein	*Embp1a*	1	pGCNN546	DraI	1/10	wheat	M. Guiltinan
NBS-LRR	*NBS-LRR.b3*	1	b3	Xba1	1/2	barley	P. Schulze-Lefert
Oxalate oxidase homologue	*Oxo1*	1	pBH6-903	DraI	3/11	barley	D. Collinge
α-Phospholipase D	*Pld*	1	pld1	EcoRI	1/2	rice	J. Leach
3D long arm							
Early-salt-induced protein	*Esi48*	1	Esi48	BamHI	1/4	*Lophopyrum elongatum*	P. Gulick
Gibberellin (GA) response complex in α-amylase gene promoter	*GAMyb*	1	HvGAmyb	HindIII	1/2	barley	F. Gabler
Proline/glycine-rich protein	*Prp*	1	pHvPRPb (pBH72-Q3)	HindIII	1/1	barley	D. Collinge
Pr4	*Pr4* (2L)	1	pBH72-B8	BamHI	2/6	barley	D. Collinge

Table 3. Continued

Gene and/or product	Symbol of the locus	No. of loci	Clone designator	Enzyme for DNA digest	No. of scored bands/total no.	Source of the clone	Supplier
4D short arm							
NBS-LRR	*NBS-LRR.b8*	1	b8	XbaI	1/4	barley	P. Schulze-Lefert
Early-salt-induced protein	*Esi3F*	1	Esi3F	BamHI	1/4	*Lophopyrum elongatum*	P. Gulick
Thaumatin	*Tha3*	1	pBH72-K10	XbaI	1/7	barley	D. Collinge
4D long arm							
Chitinase 2	*Cht21*	1	pBH72-C4	XbaI	2/2	barley	D. Collinge
Pr1a	*Pr1a*	1	pHVPr1a	XbaI	2/8	barley	D. Collinge
14-3-3 protein ion channel regulator	*1433a*	1	pHv1433a	XbaI	2/8	barley	D. Collinge
Lipoxygenase	*Lpx* (5L)	1	6CO2E12	EcoRV	4/6	maize	T. Musket
Oxalate oxidase	*Oxo2*	1	pOXOXa	BamH1	3/11	barley	D. Collinge
short arm							
long arm							
Lipoxygenase	*Lpx* (4S)	3	6CO2E12	EcoRV	4/6	maize	T. Musket
Chitinase 2	*Cht22* (1L)	1	pBH72-N12	EcoRV	2/7	barley	D. Collinge
Chalcone isomerase	*Chi* (7SC)	1	Fl19	Dra1	3/6	maize	E. Grotewold
6D short arm							
Drought and salt stress-associated protein	*WCI1*	1	WCI1	EcoRV	2/3	wheat J. Ryals	
Phenylalanine ammonia-lyase	*Pal*	1	osPAL	EcoRI	2/11	rice	E. Minamni
Cinnamyl alcohol dehydrogenase	*CAD*	1	CAD	DraI	1/7	maize	P. Puigdomenech
6D long arm							
Early-salt-induced protein	*Esi35.31*	1	Esi35.31	DraI	1/1	*Lophopyrum elongatum*	P. Gulick
NBS-LRR	*NBS-LRR.b7*	3	b7	HindIII	3/8	barley	P. Schulze-Lefert
NBS-LRR	*Rp1* (1L,2L,7L)	1	Rp1	EcoRI	4/9	maize	S. Hulbert
7D short arm							
Peroxidase	*Per*	1	6CO2D10	DraI	2/17	maize	T. Musket
Chalcone isomerase	*Chi* (5L)	2	Fl19	Dra1	3/6	maize	E. Grotewold
Proline-rich protein	*Prp2*	2	CSU133	HindIII	1/5	maize	T. Musket
Pr1b	*Pr1b*	1	pHVPr1b	DraI	2/7	barley	D. Collinge
7D long arm							
NBS-LRR	*NBS-LRR.b9* (1S)	2	b9	EcoRV	6/8	barley	P. Schulze-Lefert
NBS-LRR	*Rp1* (1L,2L,6L)	1	Rp1	EcoRI	4/9	maize	S. Hulbert

located in the subtelomeric region of 5D long arm and recombination is suppressed in the centromeric region.

Chromosome 4D is distinguished by a high rate of recombination in the subtelomeric region of the short arm only and strong suppression of recombination in 75% of its long arm. Chromosome 3D is unique in that the recombination rate of terminal/interstitial regions of short and long arms are not different from expected except for suppression of recombination in the pericentromeric region.

Chromosome 2D has a high recombination in the telomeric end of the long arm only, while recombination is suppressed in the centromeric region.

Chromosome 1D has high recombination in the telomeric end of the short arm only.

Our results lead to reject hypothesis 2, i.e. that the genetic lengths of the seven *A. tauschii* chromosomes are similar. The total genetic size of the complete maps of chromosomes 3D and 5D is not different from expected, whereas the size of 1D and 4D is smaller ($\alpha = 0.005$), and the size of 2D, 6D, and 7D is

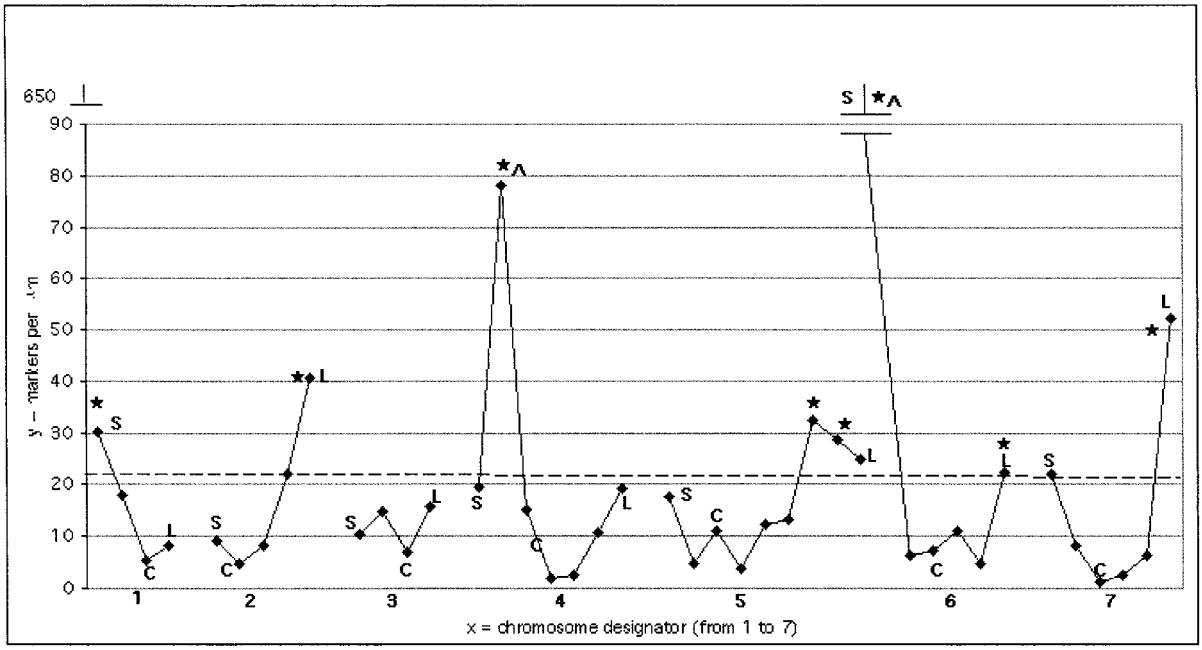

Figure 3. Physical density of markers (PD_i) in segments of *Aegilops tauschii* chromosomes. The dashed line indicates the expected PD_e in case of inter-chromosomal comparison. * and ^ indicate PDs that are different from expected in case of intra-chromosomal or inter-chromosomal comparison, respectively. S, short arm; L, long arm; C, pericentromeric region.

larger ($\alpha = 0.005$), than expected (WGRC home page, Figure 16).

Physical density of markers across the A. tauschii *genome*

The standardized physical density of markers (PD_i) was calculated for similar segments of the D-genome chromosomes of *A. tauschii* (genetic map data) and *T. aestivum* (physical map data) (Figure 3; WGRC home page, Figures 3, 5, 7, 9, 11, 13 and 15). The PD_i patterns calculated from the genetic and the physical map data are not different for individual chromosomes with the exception of selected segments on long arms of chromosomes 7D, 4D, 5D, and the telomeric segment of 6DS where the PD_i values calculated from genetic map data are different from those derived from physical maps (α is equal to 0.005, 0.05, 0.025, and 0.005, respectively; WGRC home page, Figures 9, 11, 13, and 15).

Our results do not support hypothesis 3, i.e. that the physical density of markers is uniform along the physical chromosome length. In inter-chromosomal comparisons, a region of very high marker density is located in the terminal segment of both genetic and physical maps of 6DS. A high-marker-density segment is also located in the interstitial segment of 4DS. The physical density of markers in other chromosome segments is not different from expected.

The intra-chromosomal PD_i patterns were also analyzed (Figure 3; WGRC home page, Figures 3, 5, 7, 9, 11, 13, and 15). The PD_is in the pericentromeric regions are lower but not significantly different from expected. Values of PD_i from genetic map data suggest that the physical density of markers tends to increase toward the distal and terminal chromosome regions. Also, the short and long arms of the same chromosome have different marker density. However, chromosome 3D has low overall PD_i, and arms of similar density of markers. Physical map data (WGRC home page, Figures 3, 5, 7, 9, 11, 13, and 15) indicate that chromosome segments with high PD_i are interspersed with low-density segments. Pair-wise comparisons of PD_i values for all chromosome segments are presented in Tables 3 and 4 (WGRC home page).

Hypothesis 4 stated that recombination rate and physical density of markers are correlated. A numerical descriptive measure of the association between two variables x (markers per μm) and y (cM per μm) is provided by the coefficient of correlation (r). Our results support hypothesis 4, i.e. that recombination rate and physical density of markers are strongly correlated ($r = 0.85$, $\alpha = 0.0001$; Figure 4).

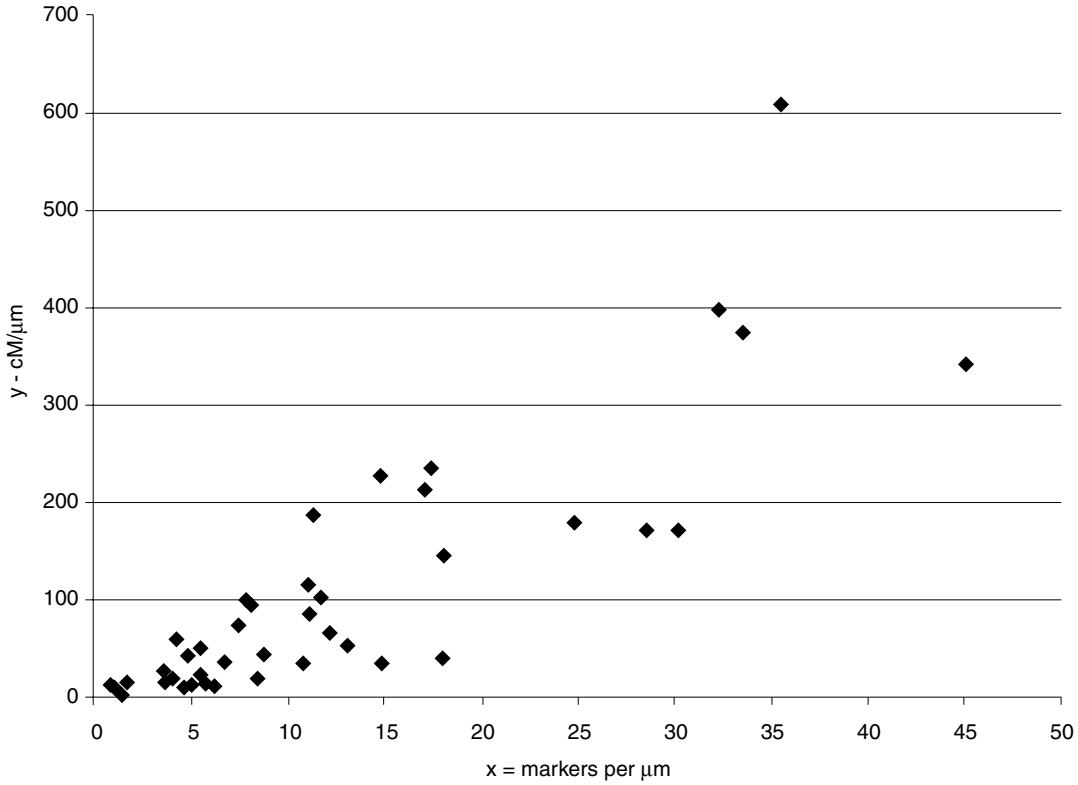

Figure 4. Correlation between physical density of markers (markers/μm) and recombination rate (cM/μm) in segments of *Aegilops tauschii* chromosomes ($r = 0.85$, $\alpha = 0.0001$).

Crossover interference

Hypothesis 5, i.e. that there is no positive or negative crossover interference in the TA1691 × TA1704 hybrid, is rejected as a result of estimates of maximum likelihood for the coefficient of coincidence (c). These results indicated that both negative and positive crossover interference (i.e., $c > 1$ and $0 < c < 1$, respectively) occurred in the genetic map of *A. tauschii* (TA1691 × TA1704) hybrid. Deviation from the 'no interference' Haldane and from Kosambi interference were highly significant. The revealed trends were confirmed by using larger intervals from one or both sides of the central point of any considered interval pair and by variation of the position of the central point.

With the exception of chromosome 7D, the remaining chromosomes showed multiple islands of positive and/or negative interference, separated from each other by zones of no interference. In some cases, islands of negative interference were adjacent to areas of positive interference (see Figure 1, chromosomes 1D, 3D, 4D, 5D, and 6D). There was no interference in interstitial and subtelotelomeric regions of 6DS and all of 7DL.

A tendency for a higher level of negative crossover interference was found in regions that were proximal to or spanned the centromere (chromosomes 2D, 3D, 4D, and 5D).

Discussion

In this paper we emphasize mapping of defense-related and retrotransposon loci and features of their distribution in the genome. We mapped 732 loci. Of these, roughly 22% (160 loci) are defense-related genes and 18% (133 loci) are retrotransposon and microsatellite markers. The remaining are anonymous genomic/cDNA probes or known gene loci. We also constructed a cytogenetic map by integrating the high-density genetic map of *A. tauschii* with the D-genome physical map of *T. aestivum*. This gives us a unique opportunity to analyze the architecture of cereal chromosomes in terms of the patterns of recombination and

Table 4. Chromosome location of clones with sequences that are similar to known resistance or defense response genes (S – short arm, C – pericentromeric region, L – long arm).

Clone name	Chromosome in location in *Ae. tauschii* (D-genome)	Similar to which known gene or gene family
KSUD14	1S	NBS-LRR
CDO99	1S	chalcone synthase
KSUG9	1S	Ca^{2+}-ATPase
ABC151	1S	lipid transfer protein gene
BCD1072	1S	heat shock protein 70
ABG373	1S	RNase S-like protein precursor
KSUM114	1L	activation factor
KSUE11	1L	disease resistance protein
KSUI27	1L	3-hydroxy-3-methylglutaryl coenzyme
KSUG30	2S	cytochrom P450
PSR109	2S, 5C	ribulose-1,5-biphosphate small subunit carboxylase
KSUD18	2S	cytosolic ascorbate peroxidase
KSUH8	2S	MYB family transcription factor
CDO64	2S, 3L, 4S	calmodulin
BCD855	2S	histone H2B promotor
KSUG57	2C, 5L	proline-rich protein
KSUF11	2C	receptor kinase 1 containing LRR
KSUD8	2L	NADH dehydrogenase subunit 5
KSUF15	2L	dihydrodipicolinate synthase
KSUM149	2L	Zink protease
KSUG5	2L	nonsense-mediated mRNA decay trans-activating factors
BCD266	2L	oryzain alpha
KSUI24	2L	extracellular transmembrane protein containing LRR
KSUF41	2L	thaumatin-like protein
BCD828	2L	ATP synthase β-subunit
KSUD53	3S	translation initiation factor
CDO395	3S	small GTP-binding protein
KSUG59	3S	catalase
KSUF34	3S	DNA helicase-primase associated protein
KSUG13	3C	DNA-binding protein
WG178	3L	homeodomain protein
KSUH2	3L	forkhead box B1a
KSUG62	3L	NBS-LRR
ABG463	4S	small GTP-binding protein
KSUF8	4S	transmembrane protein G5p
KSU114	4S	activation factor
KSUD18	4S	cytosolic ascorbate peroxidase
BCD110	4L	glycine-rich protein
KSUM147	4L	heat shock 70 kD protein
KSUG44	5S	ribulose 1,5-biphosphate carboxylase large subunit P
KSUD16	5S	E selectin
KSUA3	5C	ribulose-1,5-biphosphate carboxylase
KSUG12	5L	aspartyl t-RNA synthetase
BCD9	6S	UDP-glucose pyrophosphorilase
ABG458	6S	chlorophyll a/b binding protein
KSUI28	6S	wall-associated kinase 2
KSUD17	6L	*adh1-adh2* region
KSUE14	6L	reticulocyte-binding protein-2
KSUD1	6L	T-cell surface glycoprotein CD3
CDO836	6L	cytosolic glutathion reductase
KSUM11	6L	ABC transporter permease protein
ABC451	6L	S adenosylmethionine decarboxylase
CDO669	7S	ankyrin
BCD130	7S	lipase protein
KSUD15	7S	GTP-binding protein *OsRac3*
ABC465	7S	mRNA for sucrose synthase
CDO673	7L	allene oxydase synthase (*aos*)
KSUG49	7L	rust resistance protein *Rp1-D*
KSUG1	7L	calmodulin
KSUD9	7L	protein translation factor *Sui1*

marker density along the physical chromosome length, the relationship between recombination and physical density of markers, and the underlying phenomenon of genetic interference that may influence the rate and patterns of recombination. Before we discuss these issues in detail, several limitations of this type of data and analysis should be pointed out. First, we are able to map only polymorphic markers. Therefore, any factors that influence polymorphism such as the recent report that distal markers are more polymorphic than proximal ones will influence marker distribution patterns based on genetic mapping studies (Dvorak *et al.*, 1998). Even though this is a consideration for the *A. tauschii* genetic map, it is not for the D-genome physical map of wheat, as deletion mapping (presence/absence of a fragment) is independent of polymorphism. We also have high standard deviations (5–10%) in our calculations of deletion breakpoint positions (Endo and Gill 1996). Although this is a concern, the magnitude of differences in relative marker

and recombination distribution along the chromosome length is so large that the overall conclusions based on the cytogenetic data presented here should be valid.

Distribution of RGA and DR genes

The genes involved in resistance and defense response to pathogens are divided into two classes. These are the resistance (R) genes that are involved in the pathogen recognition process and the defense-response (DR) genes. Both types of defense-related genes are present as clusters and as single loci in *A. tauschii* chromosomes. Of the 160 mapped loci, 66 were organized into 12 clusters.

Of 111 defense-related gene probes, 44 were polymorphic. Others were identified by sequencing previously mapped markers (see Table 4). A total of 160 RGA and DR gene loci were mapped. Chromosome 2D had the most with 41 loci and 5D the fewest (14 loci). Most R and DR genes are present in multiple copies; an average of five copies for RGAs and six for DR genes. Not all of the family members were polymorphic in the parents of our mapping population – an average of 2.5 copies of RGA and 1.7 of DR genes were mapped. These results also show that polymorphism among R gene sequences is 1.8 times higher than among defense-response gene sequences. Often duplicated loci were associated with retrotransposon-based marker(s), suggesting that retrotransposons may play a role in duplication of defense-response genes. Results from the *Arabidopsis* genome sequencing project suggest that in several cases genes appear to have been included as 'passengers' in transposable units (Arabidopsis Genome Initiative, 2000).

Remarkably, the R and DR genes are organized into separate clusters consisting of one type of genes only. However, three mixed-gene clusters were observed in the distal regions of 1DL and 3DS. Clusters of RGA loci seem to coincide with various resistance phenotypes (Figure 1). Six RGA loci in the distal region of 1DS coincide with a number of known resistance genes putatively located in the same area on chromosomes 1A, 1B, and 1D of *T. aestivum*. *XksuD14*, the most distal RGA locus on 1DS is a candidate for *Lr21/Lr40* gene (Li and Gill, 2001). Defense-related loci in 2DS may be candidates for several *Lr* genes mapped in that arm (Raupp *et al.*, 2001). A cluster of six RGA loci in the distal region of 2DL (NBS-LRR family) may coincide with resistance to powdery mildew genes *Pm4* and *Pm6*. A cluster of RGA loci may coincide with one of the several resistance genes in the distal region of 7DL. There are also RGA loci in the genetic map that do not correspond to any known resistance gene in the physical map, and vice versa (Figure 1). We suggest that these sites might possibly be the location of unidentified resistance or unmapped R gene clusters.

Although there are limitations to the data as all mapped probes have not been sequenced, there is a clear trend showing that R-gene loci tend to be located in the telomeric regions. Thus R gene loci are located at or near telomeric ends in 1D, 3DS, 4DS, 6DL, and 7D. Similarly, one or more DR loci are located in terminal ends of 1DL, 2D, 3D, and 6DL. Chromosome 2D appears to be exceptional where R-gene loci map more proximally as compared to DR loci. However, in general, DR loci have a more proximal location than R loci. The cytogenetic maps presented here clearly show that recombination is extremely high at the telomeric ends. Thus, the location of R genes and some of the DR genes in high recombination regions may be responsible for their high rate of evolution (see below) to defend the plants in a co-evolutionary race against rapidly evolving pathogen populations.

Based on sequence similarity among members of the same cluster, homogenic and/or heterogenic clusters of R genes were reported in lettuce (Kesseli *et al.*, 1993; Sicard *et al.*, 1999), common bean (Creusot *et al.*, 1999; Geffroy *et al.*, 1999; Rivkin *et al.*, 1999), soybean (Kanazin *et al.*, 1996), flax (Ellis *et al.*, 1999), and *Arabidopsis* (Noël *et al.*, 1999). In *A. tauschii*, clusters of highly dissimilar R-gene-related sequences are found in the distal region of 1DS (*XECD10, XNBS-LRR.b6*, and *XNBS-LRR.b9* loci). A cluster of similar RGA sequences interrupted with anonymous RFLP loci and NBS-LRR type sequence from maize (*XRp1*) mapped to the distal region of 2DL. Some of the R-gene-related sequences were mapped as single loci (see Figure 1 and Table 3). Because average of only 56% of bands from Southern hybridization autoradiograms of R gene were polymorphic (Table 3), we believe that these single loci represent R gene clusters that are yet to be mapped.

Some of the RGAs that were used in this study were also mapped in wheat, rice (*Oryza sativa*), barley, and foxtail millet (*Setaria italica*) (Feuillet and Keller 1999; Spielmeyer *et al.*, 1998; Leister *et al.*, 1998, 1999). Comparisons of our map and published maps revealed both syntenic and nonsyntenic map positions of common RGA loci (Table 5). Syntenic loci might represent orthologous sequences of R-genes in the genome(s) of the common ancestor(s) of the Trit-

iceae (barley and wheat), Oryzeae (rice), and Paniceae (foxtail millet) tribes. The *NBS-LRR.b1* (*A. tauschii* and foxtail millet) and *NBS-LRR.b9* (*A. tauschii*, barley, rice, and foxtail millet) are syntenic in the grasses and may be assumed to be the most ancestral and conserved among the analyzed RGA sequences. The *NBS-LRR.b4* and *NBS-LRR.r4* loci were located in syntenic regions in *A. tauschii* and rice. Non-syntenic locations of R genes (Table 5) might reflect the lack of mapping data available for the species mentioned above or arise from duplication events followed by loss of the original R loci.

Only one of 16 rice RGAs was mapped in *A. tauschii*. All the other rice RGA probes gave a smeared hybridization pattern suggesting a highly repetitive nature of *A. tauschii* sequences homologous to rice RGAs. This result is in agreement with reports that R genes are highly diverse and evolving rapidly by gene duplication, diversification, and subsequent selection (Geffroy *et al.*, 1999; Noël *et al.*, 1999). Yet, our results suggest that only a part of R genes are evolving rapidly, whereas other R-gene sequences share high sequence similarity among the different taxa of the Gramineae.

Distribution of retrotransposon and microsatellite markers

Retrotransposon-marker systems are based on primers targeting the long terminal repeats (LTRs) of particular retrotransposons. The development of marker and fingerprint methods based on LTR-retrotransposons has been largely confined to barley (Waugh *et al.*, 1997; Kalendar *et al.*, 1999) until now. In principle, extension of the approach to other species is possible if the retrotransposons are sufficiently dispersed and have good polymorphism and map coverage. The LTR primers from one retrotransposon family, such as *BARE*-1, can be applied directly in a heterologous species if the LTRs of related elements in that species are sufficiently conserved and the insertion sites polymorphic (Vicient *et al.*, 2001). Alternatively, LTRs from the new species may be isolated by generic methods relying on conserved domains within retrotransposons (Pearce *et al.*, 1999). In a previous study (Gribbon *et al.*, 1999), the *BARE*-1 LTR primers were sufficiently conserved to yield marker bands with the SSAP method, which is in essence an anchored AFLP approach (Waugh *et al.*, 1997) combining a REMAP-type outward-facing primer with an AFLP-type adapter primer. In the present study, both the *BARE*-1 and *Sukkula* (another LTR-retrotransposon in barley) primers served well for mapping.

A particular feature of the retrotransposon loci mapped here is their occasional local clustering. The largest cluster is of eight REMAP loci mapped in the pericentromeric region of 5D; others were observed on 1D, 6D, and 7D. However, the retrotransposon markers as a whole are dispersed on all chromosomes, in agreement with previous *in situ* hybridization results (Suoniemi *et al.*, 1996a; Vicient *et al.*, 1999). The clustering of *BARE*-1 markers has been observed previously with both SSAP (Waugh *et al.*, 1997) and REMAP and IRAP (Manninen *et al.*, 2000) markers in barley. Most likely, this phenomenon is related to the fact that a number of the grass genomes are structured as 'gene islands surrounded by repeat seas' (Panstruga *et al.*, 1998). The apparent tendency of *BARE*-1 retrotransposons is to insert near microsatellite domains (Kalendar *et al.*, 1999; Ramsay *et al.*, 1999; this study). The nested insertion of BARE-1 and other retrotransposons within the genome is also noted (Shirasu *et al.*, 2000). Nevertheless, because the gene islands themselves may be small and are not fully retrotransposon-free (Shirasu *et al.*, 2000), retrotransposon markers remain useful for recombinational mapping of traits (Manninen *et al.*, 2000).

Retrotransposon clusters coincide with areas of lower recombination rate in all chromosomes. This can be clearly seen in pericentromeric regions of cytogenetic maps of chromosomes 1D, 5D, 6D, and 7D. In chromosome 1D, most retrotransopon loci lie in a pericentromeric region encompassing 50% of the short arm and 40% of the long arm (see 1D consensus map in Figure 1). The genetic length of this region is only a few centimorgans (see corresponding region of 1D genetic map in Figure 1). In 5D, retrotransposon loci are clustered in the pericentromeric region. It consists of 20% of short arm and 29% of long arm (see 5D physical map in Figure 1) that covers a genetic length of only a fraction of the entire map length of 5D. In chromosomes 6D and 7D also, clustering of retrotransposon loci is associated with regions of suppressed recombination. Conversely, retrotransposon loci are more frequent in distal regions of 4DS and 7DS arms that have greatly reduced rates of recombination. A similar observation was made in *Arabidopsis*, where high transposon density coincided with regions of low recombination (Arabidopsis Genome Initiative, 2000). One may speculate that genetic mechanisms that led to the silencing of transposable elements also caused reduced recombination. As 70% of the wheat genome

Table 5. Chromosome locations of resistance gene analogs mapped in this study and previously published.

Symbol of the locus	Chromosome location				
	Aegilops tauschii	*Triticum aestivum*	*Hordeum vulgare*	*Oryza sativa*	*Setaria italica*
ECD10	1DS	1AS* 1HS*			
NBS-LRR.b9	1DS,7DS, 7DL	4DL**	7HS***	1(3), 2(6), 8(7S)***	VIII(5, 6L), VI(7S), V(3S)***
NBS-LRR.b6	1DS		1HS, 3HS***	11(6L), 8(7S)***	
NBS-LRR.b4	1DL			5(1L)***	
Rp1	1DL, 2DL, 6DL, 7DL	1DL, 3DL, 4DL**			
NBS-LRR.b1	2DL				VII(2L)***
NBS-LRR.r1	2DL			4(2L), 11(6)***	
NBS-LRR.b5	2DL	1AS, 1BS, 1DS**			
NBS-LRR.b8	4DS		5HL***	5(1L), 11(6L)***	
NBS-LRR.b7	6DL	6DL**	1HS, 6HL***		V(3L)***
NBS-LRR.b3	6DL		3HS, 3HL, 4H***		

*Feuillet and Keller, 1999.
**Spielmeyer *et al.*, 1998.
***Leister *et al.*, 1998, 1999.

consists of retro elements (Wicker *et al.*, 2001), it is also possible that reduced gene density in transposon-rich regions may indirectly lead to reduced recombination as recombination occurs preferentially in gene rich regions (see Schnable *et al.*, 1998, for review).

Of the 50 D-genome microsatellite markers, 40 were polymorphic and 31 were integrated into the map of *A. tauschii*. The number of microsatellite markers per chromosome ranged from one on 7D to eight on 2D. The position of most microsatellite markers in *Aegilops tauschii* was similar to the D-genome map of hexaploid bread wheat as described by Röder *et al.* (1998). In general, microsatellites were dispersed all over the genome and in many cases, they mapped in or near R, DR, and retrotransposon-gene clusters (Figure 1).

The distribution of recombination

Information about recombination rates was obtained from an analysis of genetic versus physical length values in various chromosome segments (Figure 2; WGRC home page, Figures 2, 4, 6, 8, 10, 12, and 14). Pericentromeric and/or interstitial regions of seven *A. tauschii* chromosomes showed suppression of recombination, with the lowest values in most segments of 4D, 6D, and 7D. Regions with low recombination rates were near segments with high recombination rates located in distal and terminal regions of both chromosome arms. A 'burst' of recombination was detected in the terminal and distal regions of 6DS and 7DL, respectively (values were 2.2 and 1.5 times higher than the nearest recombination rate value, respectively). In general, recombination rate appears to be significantly less than expected in pericentromeric regions, and higher than expected in subtelomeric regions of both chromosome arms. A similar pattern was discovered in human chromosomes, where the recombination rate was evaluated as cM per Mb calculated in 3 Mb windows (Venter *et al.*, 2001; Yu *et al.*, 2001).

The rate of recombination for each chromosome and of its short and long arms was unique and may reflect the individual history of its sequence evolution. The genetic lengths of 3D and 5D chromosomes of *A. tauschii* are different from each other but not different from expected. Chromosome 1D is not different from 4D, but the total genetic length is less than expected. The genetic maps of 2D, 6D, and 7D are longer than expected but are different from one another (WGRC home page, Figure 16), suggesting that different chromosomes and different arms of the same chromosome have different recombination frequencies.

Physical density of markers

The physical density of markers also is not uniform along *A. tauschii* chromosomes (Figure 3; WGRC

home page, Figures 3, 5, 7, 9, 11, 13, and 15) and differs among chromosome arms. It is the lowest in pericentromeric regions of all seven *A. tauschii* chromosomes and is higher toward telomeric regions often interrupted by areas of low marker density. For most chromosome segments, the physical density of markers calculated using genetic map data (PD_{ig}) is not significantly different from that calculated for the same segments using physical map data (PD_{ip}). This result suggests that we divided the genetic map into segments that precisely correspond to segments on the physical map, and that the D-genome of bread wheat and of *A. tauschii* maintained similar patterns of distribution of genes and other sequences. Chromosome 3 had a below-average overall marker density. All chromosomes had unique distribution patterns of marker density, even though the general pattern of higher densities in distal and lower density in proximal chromosome areas is maintained. Another distinctive feature of chromosome organization was that regions of high marker density were interspersed with regions of low marker density even in the distal and interstitial parts of *A. tauschii* chromosomes. Recently, Wicker *et al.* (2001) sequenced a 211 kb contiguous piece of DNA in wheat; it contained five genes, three of which clustered on a 31 kb gene-rich island. In *Arabidopsis*, the gene density gradually decreases towards the pericentromeric/centromeric region (European Union Chromosome 3 *Arabidopsis* Sequencing Consortium *et al.*, 2000). The human genome also consists of gene-rich and gene-poor regions that are non-randomly distributed over the various human chromosomes (Venter *et al.*, 2001).

Correlation between physical marker density and recombination rates

The patterns of PD_i and recombination rate are similar and show a strong correlation ($r = 0.849$, $\alpha = 0.0001$, Figure 4). This indicates that chromosome regions with a higher concentration of markers have more crossovers. Because most of the mapped markers represent functional gene sequences, one may suggest that recombination is more likely to occur in gene-rich regions. Previously, Gill *et al.* (1996a, b) also demonstrated a correlation between marker density and recombination. Wicker *et al.* (2001) sequenced a 211 kb wheat DNA and localized recombination events in the gene island region to a 2.5 kb interval containing a microsatellite and a direct repeat element. Spielmeyer *et al.* (2000) reported a ratio of 20 kb/cM in the 1DS cluster around the *Gli-D1* locus of *A. tauschii*. A similar trend has been reported in the human and *Arabidopsis* genomes (Kazusa DNA Research Institute *et al.*, 2000; European Union Chromosome 3 Arabidopsis Sequencing Consortium *et al.*, 2000; Yu *et al.*, 2001; Caron *et al.*, 2001; International Human Genome Sequencing Consortium, 2001; Venter *et al.*, 2001).

Structural rearrangements of the genome

There are significantly low recombination rates in areas other than proximal that coincide with regions on the genetic map where the order of markers is different from that of the D-genome physical map. A comparison of the physical maps of *T. aestivum* D-genome chromosomes and genetic maps of *A. tauschii* chromosomes showed a different marker order in some chromosomes (see Figure 1, chromosomes 3, 4, 5, and 7). In the chromosome 3D short arm, the order of loci *XksuI32/XksuF34* and *Xglk724* is reversed in the genetic and physical maps. In chromosome 4D, loci *Xpsr157* and *Xcdo1387* were mapped in the short arm in genetic map of *A. tauschii*, but were located in the FL 0.46–0.53 interval in the long arm in the *T. aestivum* physical map. A *T. aestivum* chromosome 4D short-arm marker *Xpsr139* (FL 0.63–0.67) is mapped to the long arm in the *A. tauschii* genetic map. Two thirds of both chromosome arms also had significantly suppressed recombination (Figure 2). We localized the centromere on the *A. tauschii* genetic map (assuming it is located between the same markers as on the physical map) and calculated the genetic length for both arms of 4D. The short arm was significantly longer ($\alpha = 0.005$) than the long arm and had almost twice the number of markers. The number of short-arm markers was half the number of long-arm markers on the *T. aestivum* 4D physical map. See also the reverse order of markers on 5DL and 7DS cytogenetic maps. These results suggest that the parents of the mapping population are either heterozygous or fixed for inversions and other structural aberrations involving small chromosome segments where recombination is suppressed. However, Friebe *et al.* (1992) observed very few obvious structural changes in a survey of *A. tauschii* germplasm by C-banding and also in a meiotic analysis of the F_1 hybrid (TA1991/TA1704) used for genetic mapping in the present study.

Negative crossover interference

Positive crossover interference, i.e., a reduced frequency of adjacent crossovers compared to that expected under an assumption of independence, is a characteristic of meiotic organisms, with only a very few exceptions (Egel-Mitani *et al.*, 1982). However, we found a significant excess of double exchanges in segments spanning or proximal to the centromere and/or located in distal and interstitial regions of both arms in nearly all chromosomes of *A. tauschii*. Alternating areas of strong negative and positive interference, both interrupted by regions of no interference, were demonstrated. Similar results were reported for the A and B genomes of *T. diccocoides* (Peng *et al.*, 2000). An overall comparison of the number of markers showing negative, positive, or no interference suggests their random distribution among the chromosomes with the exception of 5D, which had a higher than average number of markers with positive or no interference ($\alpha = 0.005$). The total number of markers that showed positive interference was half that ($\alpha = 0.001$) of markers with negative interference. The number of markers with negative interference was similar to that with no interference. The distribution of markers with negative, positive or no interference did not show a random pattern when telomeric + interstitial (TI) and pericentromeric regions were compared. Half of the markers with negative or no interference, and 90% of those with positive interference were located in the TI regions of the long arms.

When the numbers of markers with different interference effects are compared in each region mentioned above, different patterns are revealed: a lack of positive interference and an equal number of negative and no-interference markers in the TI regions of the short arm (3%, 44%, and 54% out of total number of markers mapped in the region, respectively); a prevalence of negative interference over the other two types of markers in pericentromeric region (80% over (10+10)%, respectively); and equal numbers of all three types of markers located in the long arm TI regions. The highest concentration of negative interference in the proximal region of both arms that accounts for about 13–26% of the chromosome's cytological length but only 2–6% of the genetic length, is in agreement with data obtained for *Drosophila melanogaster*. In that species, within a 4 cM long segment accounting for about 25% of the cytological length of chromosome 3 and spanning the centromere, a significant excess of multiple exchanges was found (Sinclair, 1975). Similar results have been obtained in other *Drosophila* studies with autosomes (Green, 1975; Denell and Keppy, 1979; Korol *et al.*, 1994), but not with the X-chromosome (Lake, 1986). A significant excess of double exchanges in segments spanning or proximal to the centromere was found in nearly all chromosomes of the A and B genomes of *T. diccocoides* (Peng *et al.*, 2000).

The observed distribution of islands of negative interference (proximal of both arms and/or interstitial/subterminal) and the alternating positive/negative/no-interference can be explained by two possible models: (1) based on the hypothesis of Denell and Keppy (1979), negative interference could be a characteristic of regions with a low density of recombination per unit physical length, and (2) based on recent findings in cereal genomics (Gill *et al.*, 1996a, b; Panstruga *et al.*, 1998, Kunzel *et al.*, 2000), gene-rich segments in wheat and barley chromosomes have a higher recombination rate than gene-poor segments. Our results favor the first hypothesis. The pericentromeric region of D-genome chromosomes had strong negative interference and the lowest recombination per physical length (recombination rate). This region also has the lowest physical density of markers. We suggest that negative interference could be typical of all regions exhibiting a low density of markers and recombination per unit physical length. In this case, single crossovers, on a scale of physical distance, are manifested as double crossovers on the scale of genetic distance. Sybenga (1996) proposed that negative interference could be due to small interruptions of homology disturbing synaptonemal complex formation and thus blocking interference.

We cannot completely reject the second hypothesis. The presence of islands of 'positive-negative interference' in chromosome segments that have higher recombination rates and physical densities of markers may suggest that more than the expected number of double crossovers occurred within the gene-rich islands and recombination within an island reduces the chance of crossover in adjacent gene-poor segments.

Cereal chromosome model

From the cytogenetic maps described here, the emerging model of chromosome structure and function of cereals with large genomes may be depicted as follows. There is a clear structural and functional differentiation along the centromere/telomere axis. The pericentromeric region has low marker density and

correlated suppressed recombination accompanied by negative interference, and clustering of retrotransposon loci. Thus, as 70% of the wheat genome may consist of retrotransposons (Wicker *et al.*, 2001), most of the genome expansion probably occurred in the pericentromeric regions. In contrast, the distal regions invariably have high marker density and correlated high recombination associated with islands of positive, negative or no interference. Most of the useful genes including R and DR genes are clustered in distal/telomeric regions. However, as is true with any biological system, there are exceptions indicative of the dynamic nature of the genome including numerous structural rearrangements as documented by the cytogenetic maps of chromosomes 3D, 4D, 5D, and 7D. In fact, certain retrotransposon loci and microsatellites seem to be preferentially located in gene island regions as shown in the maps here and documented by DNA sequence analysis (Wicker *et al.*, 2001).

Acknowledgements

This work is contribution 02-78-J from the Kansas Agricultural Experimental Station, Kansas State University, Manhattan, KS. This research was supported by a special United States Department of Agriculture (USDA) grant to the Wheat Genetics Resource Center (WGRC) at Kansas State University. We thank J.C. Nelson and W.J. Raupp for useful discussions regarding data analysis and manuscript preparation.

References

Arabidopsis Genome Initiative. 2000. Analysis of the genome sequence of the flowering plant *Arabidopsis thaliana*. Nature 408: 796–815.

Arumuganathan, K. and Earle, E.D. 1991. Nuclear DNA content of some important plant species. Plant Mol. Biol. Rep. 9: 208–218.

Bennett, M.D. and Leitch, I.J. 1995. Nuclear DNA amounts in Angiosperms. Ann. Bot. 76: 113–176.

Boyko, E.V., Gill, K.S., Mickelson-Young, L., Nasuda, S., Raupp, W.J., Ziegle, J.N., Singh, S., Hassawi, D.S., Fritz, A.K., Namuth, D., Lapitan, N.L.V. and Gill, B.S. 1999. A high-density genetic linkage map of *Aegilops tauschii*, the D-genome progenitor of bread wheat. Theor. Appl. Genet. 99: 16–26.

Bryngelsson, T., Sommer-Knudsen, J., Gregersen, P.L., Collinge, D.B., Ek, B. and Thordal-Christensen, H. 1994. Purification, characterization, and molecular cloning of basic PR-1-type pathogenesis-related proteins from barley. Mol. Plant-Microbe Interact. 7: 267–275.

Caron, H., van Schaik, B., van der Mee, M., Baas, F., Riggins, G., van Sluis, P., Hermus, M.-C., van Asperen, R., Boon, K., Voute, P.A., Heisterkamp, S., van Kampen, A. and Versteeg, R. 2001. The human transcriptome map: clustering of highly expressed genes in chromosomal domains. Science 291: 1289–1292.

Collins, N.C., Webb, C.A., Seah, S., Ellis, J.G., Hulbert, S.H. and Pryor, A. 1998. The isolation and mapping of disease resistance gene analogs in maize. Mol. Plant-Microbe Interact. 11: 968–978.

Creusot, F., Macadré, C., Ferrier Cana, E., Riou, C., Geffroy, V., Sévignac, M., Dron, M. and Langin, T. 1999. Cloning and molecular characterization of three members of the NBS-LRR subfamily located in the vicinity of the *Co-2* locus for anthracnose resistance in *Phaseolus vulgaris*. Genome 42: 254–264.

Delaney, D.E., Nasuda, S., Endo, T.R., Gill, B.S. and Hulbert, S.H. 1995a. Cytologically based physical maps of the group-2 chromosomes of wheat. Theor. Appl. Genet. 91: 568–573.

Delaney, D.E., Nasuda, S., Endo, T.R., Gill, B.S. and Hulbert, S.H. 1995b. Cytologically based physical maps of the group-3 chromosomes of wheat. Theor. Appl. Genet. 91: 780–782.

Denell, R.E. and Keppy, D.O. 1979. The nature of genetic recombination near the third chromosome centromere of *Drosophila melanogaster*. Genetics 93: 117–130.

Dvorák, J., Luo, M.-C., Yang, Z.-L. 1998. Restriction fragment length polymorphism and divergence in the genomic regions of high and low recombination in self-fertilizing and cross-fertilizing *Aegilops* species. Genetics 148: 423–434.

Egel-Mitani, M., Olsson, L.W. and Egel, R. 1982. Meiosis in *Aspergillus nidulans*: another example for lacking synaptonemal complexes in the absence of crossover interference. Hereditas 97: 179–187.

Ellis, J.G., Lawrence, G.J., Luck, J.E. and Dodds, P.N. 1999. Identification of regions in alleles of the flax rust resistance gene *L* that determine differences in gene-for-gene specificity. Plant Cell 11: 495–506.

Endo, T.R. and Gill, B.S. 1996. The deletion stocks of common wheat. J. Hered. 87: 295–307.

European Union Chromosome 3 Arabidopsis Sequencing Consortium and Institute for Genomic Research and Kazusa DNA Research Institute. 2000. Sequence and analysis of chromosome 3 of the plant *Arabidopsis thaliana*. Nature 408: 820–822.

Ewing, B. and Green, P. 1998. Base-calling of automated sequencer traces using phred. II. Error probabilities. Genome Res. 8: 186–194.

Ewing, B., Hillier, L., Wendl, M.C., and Green, P. 1998. Base-calling of automated sequencer traces using phred. I. Accuracy assessment. Genome Res. 8: 175–185.

Faris, J.D., Li, W.L., Liu, D.J., Chen, P.D. and Gill, B.S. 1999. Candidate gene analysis of quantitative disease resistance in wheat. Theor. Appl. Genet. 98: 219–225.

Feuillet, C. and Keller, B. 1999. High genome density is conserved at syntenic loci of small and large grass genomes. Proc. Natl. Acad. Sci. 96: 8265–8270.

Flavell, A.J., Knox, M.R., Pearce, S.R. and Ellis, T.H.N. 1998. Retrotransposon-based insertion polymorphisms (RBIP) for high through-put marker analysis. Plant J. 16: 643–650.

Friebe, Mukai Y. ans Gill B.S. 1992. C-banding polymorphism in several accessions of *Triticum tauschii*. Genome 35: 192–199.

Geffroy, V., Sicard, D., de Olivera, J.C.F., Sévignac, M., Cohen, S., Gepts, P., Neema, C., Langin, T. and Dron, M. 1999. Identification of an ancestral resistance gene cluster involved in the coevolution process between *Phaseolus vulgaris* and its fungal pathogen *Colletotrichum lindemuthianum*. Mol. Plant-Microbe Interact. 12: 774–784.

Gill, B.S., Friebe, B. and Endo, T.R. 1991a. Stardard karyotype and nomenclature system for description of chromosome bands and

structural aberrations in wheat (*Triticum aestivum*). Genome 34: 830–839.

Gill, K.S., Lubbers, E.L., Gill, B.S., Raupp, W.J. and Cox, T.S. 1991b. A genetic linkage map of *Triticum tauschii* (DD) and its relationship to the D genome of bread wheat (AABBDD). Genome 34: 362–374.

Gill, K.S., Gill, B.S. and Endo, T.R. 1993. A chromosome region-specific mapping strategy reveals gene-rich telomeric ends in wheat. Chromosoma 102: 374–381.

Gill, K.S., Gill, B.S., Endo, T.R. and Boyko, E.V. 1996a. Identification and high-density mapping of gene-rich regions in chromosome group 5 of wheat. Genetics 143: 1001–1012.

Gill, K.S., Gill, B.S., Endo, T.R. and Taylor, T. 1996b. Identification and high-density mapping of gene-rich regions in chromosome group 1 of wheat. Genetics 144: 1883–1891.

Gordon, D., Abajian, C., and Green, P. 1998. Consed: a graphical tool for sequence finishing. Genome Res. 8: 195–202.

Green, M.M. 1975. Conversion as a possible mechanism of high coincidence values in the centromere region of *Drosophila*. Mol. Gen. Genet. 139: 57–66.

Gribbon, B.M., Pearce, S.R., Kalendar, R., Schulman, A.H., Jack, P., Kumar, A. and Flavell, A.J. 1999. Phylogeny and transpositional activity of *Ty1-copia* group retrotransposons in cereal genomes. Mol. Gen. Genet. 261: 883–891.

Hohmannn, U., Endo, T.R., Gill, K.S. and Gill, B.S. 1994. Comparison of genetic and physical maps of group-7 chromosomes from *Triticum aestivum* L. Mol. Gen. Genet. 245: 644–653.

International Human Genome Sequencing Consortium 2001. Initial sequencing and analysis of the human genome. Nature 409: 860–920.

Jääskeläinen, M., Mykkänen, A-H., Arna, T., Vicient, C., Suoniemi, A., Kalendar, R., Savilahti, H. and Schulman, A.H. 1999. Retrotransposon *BARE*-1: expression of encoded proteins and formation of virus-like particles in barley cells. Plant J. 20: 413–422.

Kalendar, R., Grob, T., Regina, M., Suoniemi, A. and Schulman, A.H. 1999. IRAP and REMAP: two new retrotransposon-based DNA fingerprinting techniques. Theor. Appl. Genet. 98: 704–711.

Kalendar, R., Tanskanen, J., Immonen, S., Nevo, E. and Schulman, A.H. 2000. Genome evolution of wild barley (*Hordeum spontaneum*) by *BARE*-1 retrotransposon dynamics in response to sharp microclimatic divergence. Proc. Natl. Acad. Sci. USA 96: 6603–6607.

Kam-Morgan, L.N.W., Gill, B.S. and Muthukrishnan, S. 1989. DNA restriction fragment length polymorphisms: a strategy for genetic mapping of D genome of wheat. Genome 32: 724–732.

Kanazin, V., Marek, L.F. and Shoemaker, R.C. 1996. Resistance gene analogs are conserved and clustered in soybean. Proc. Natl. Acad. Sci. USA 93: 11746–11750.

Kazusa DNA Research Institute, Cold Spring Harbor Laboratory, Washington University in St. Louis Sequencing Consortium, and European Union Arabidopsis Genome Sequencing Consortium. 2000. Sequence and analysis of chromosome 5 of the plant *Arabidopsis thaliana*. Nature 408: 823–826.

Kesseli, R., Witsenboer, H., Stanghellini, M., Vandermark, G. and Michelmore, R. 1993. Recessive resistance to *Plasmopara lactucae-radicis* maps by bulked segregant analysis to a cluster of dominant disease resistance genes in lettuce. Mol. Plant-Microbe Interact. 6: 722–728.

Korol, A.B., Preygel, I.A. and Preygel, S.I. 1994. Recombination Variability and Evolution Algorithms of Estimation and Population Genetics Models. Chapman and Hall, London.

Kumar, A. and Bennetzen, J. 1999. Plant retrotransposons. Annu. Rev. Genet. 33: 479–532.

Kunzel, G., Korzun, L., and Meister A. 2000. Cytologically integrated physical RFLP maps for the barley genome based on translocation breakpoints. Genetics 154: 397–412.

Lake, S. 1986. Recombination frequencies and the coincidence in proximal X-chromosome regions including heterochromatin in *Drosophila melanogaster*. Hereditas 105: 263–268.

Lander, E.S., Green, P., Abrahamson, J., Barlow, A., Daly, M.J., Lincoln, S.E. and Newburg, L. 1987. MAPMAKER: an interactive computer package for constructing primary genetic linkage maps of experimental and natural populations. Genomics 1: 81–181.

Leister, D., Kurth, J., Laurie, D.A., Yano, M., Sasaki, T., Devos, K., Graner, A. and Schulze-Lefert, P. 1998. Rapid reorganization of resistance gene homologues in cereal genomes. Proc. Natl. Acad. Sci. USA 95: 370–375.

Leister, D., Kurth, J., Laurie, D.A., Yano, M., Sasaki, T., Graner, A. and Schulze-Lefert, P. 1999. RFLP and physical mapping of resistance gene homologues in rice (*O. sativa*) and barley (*H. vulgare*). Theor. Appl. Genet. 98: 509–520.

Li, H. and Gill, B.S. 2001. An RGA-like marker detects all known *Lr21* leaf rust resistance gene family members in *Aegilops tauschii* and wheat. Theor. Appl. Genet., in press.

Li, W.L., Faris, J.D., Chittoor, J.M., Leach, J.E., Hulbert, S.H., Liu, D.J., Chen, P.D. and Gill, B.S. 1999. Genomic mapping of defense response genes in wheat. Theor. Appl. Genet. 98: 226–233.

Manninen, O., Kalendar, R., Robinson, J. and Schulman, A.H. 2000. Application of *BARE*-1 retrotransposon markers to map a major resistance gene for net blotch in barley. Mol. Gen. Genet. 264: 325–334.

Matsuoka, Y. and Tsunewaki K. 1996. Wheat retrotransposon families identified by reverse transcriptase domain analysis. Mol. Biol. Evol. 13: 1384–1392.

McClave, J.T. and Dietrich, F.H. II. 1982. Statistics. Dellen Publishing Company, San Francisco/Santa Clara, CA, 766 pp.

Mickelson-Young, L., Endo, T.R. and Gill, B.S. 1995. A cytogenetic ladder-map of the wheat homoeologous group-4 chromosomes. Theor. Appl. Genet. 90: 1007–1011.

Muthukrishnan, S., Liang, G.H., Trick, H.N. and Gill B.S. 2001. Pathogenesis-related proteins and their genes in cereals. Plant Cell Tissue Organ Cult. 64: 93–114.

Noël, L., Moores, T.L., van der Biezen, E.A., Parniske, M., Daniels, M.J., Parker, J.E. and Jones, J.D.G. 1999. Pronounced intraspecific haplotype divergence at the *RPP5* complex disease resistance locus of *Arabidopsis*. Plant Cell 11: 2099–2111.

Panstruga, R., Büschges, R., Piffanelli, P. and Schulze-Lefert, P. 1998. A contiguous 60 kb genomic stretch from barley reveals molecular evidence for gene islands in a monocot genome. Nucl. Acids Res. 26: 1056–1062.

Pearce, S.R., Harrison, G., Heslop-Harrison, J.S., Flavell, A.J. and Kumar, A. 1997. Characterization and genomic organization of *Ty1-copia* group retrotransposons in rye (*Secale cereale*). Genome 40: 1–9.

Pearce, S.R., Stuart-Rogers, C., Knox, M.R., Kumar, A., Noel-Ellis, T.H. and Flavell, A.J. 1999. Rapid isolation of plant *Ty1*-copia group retrotransposon LTR sequences for molecular marker studies. Plant J. 19: 711–717.

Peng, J., Korol, A.B., Fahima, T., Röder, M.S., Ronin, Y.I., Li, Y.C. and Nevo, E. 2000. Molecular genetic maps of wild emmer wheat, *Triticum diccocoides*: genome-wide coverage, massive negative interference, and putative quasi-linkage. Genome Res. 10: 1509–1531.

Plaschke, J., Börner, A., Wendehake, K., Ganal, M.W. and Röder, M.S. 1996. The use of wheat aneuploids for the chromosomal assignment of microsatellite loci. Euphytica 89: 33–40.

Ramsay, L., Macaulay, M., Carle, L., Morgante, M., Degli-Ivanissevich, S., Maestri, E., Powell, W. and Waugh, R. 1999. Intimate association of microsatellite repeats with retrotransposons and other dispersed repetitive elements in barley. Plant J. 17: 415–425.

Raupp, W.J., Singh, S., Brown-Guedira, G.L. and Gill, B.S. 2001. Cytogenetic and molecular mapping of the leaf rust resistance gene *Lr39* in wheat. Theor. Appl. Genet. 102: 347–352.

Rivkin, M.I., Vallejos, C.E. and McClean, P.E. 1999. Disease-resistance related sequences in common bean. Genome 42: 41–47.

Röder, M.S., Plaschke, J., König, S.U., Börner, A., Sorrells, M.E., Tanksley, S.D. and Ganal, M.W. 1995. Abundance, variability and chromosomal location of microsatellites in wheat. Mol. Gen. Genet. 246: 327–333.

Röder, M.S., Korzun, V., Wendehake, K., Plaschke, J., Tixier, M-H., Leroy, P. and Ganal, M.W. 1998. A microsatellite map of the wheat genome. Genetics 149: 2007–2023.

Sandhu, D., Champoux, J.A., Bondareva, S.N. and Gill, K.S. 2001. Identification and physical localization of useful genes and markers to a major gene-rich region on wheat group 1S chromosomes. Genetics 157: 1735–1747.

Schnable, P.S., Hsia, A.P. and Nikolau, B.J. 1998. Genetic recombination in plants. Curr. Opin. Plant Biol. 1(2): 123–129.

Seah, S., Sivasithamparam, K., Karakousis, A. and Lagudah, E.S. 1998. Cloning and characterization of a family of disease resistance gene analogs from wheat and barley. Theor. Appl. Genet. 97: 937–945.

Seah, S., Spielmeyer, W., Jahier, J., Sivasithamparam, K. and Lagudah, E.S. 2000. Resistance gene analogs within an introgressed chromosomal segment derived from *Triticum ventricosum* that confers resistance to nematode and rust pathogens in wheat. Mol. Plant-Microbe Interact. 13: 334–341.

Shirasu, K., Schulman, A.H., Lahaye, T. and Schulze-Lefert, P. 2000. A contiguous 66 kb barley DNA sequence provides evidence for reversible genome expansion. Genome Res. 10: 908–915.

Sicard, D., Woo, S.-S., Arroyo-Garcia, R., Ochoa, O., Nguyen, D., Korol, A., Nevo, E. and Michelmore, R. 1999. Molecular diversity at the major cluster of disease resistance genes in cultivated and wild *Lactuca* ssp. Theor. Appl. Genet. 99: 405–418.

Sinclair, D.A. 1975. Crossing over between closely linked markers spanning the centromere of chromosome 3 in *Drosophila melanogaster*. Genet. Res. 11: 173–185.

Spielmeyer, W., Robertson, M., Collins, N., Leister, N., Schulze-Lefert, P., Seah, S., Moullet, O. and Lagudah, E.S. 1998. A superfamily of disease resistance gene analogs is located on all homoeologous groups of wheat (*Triticum aestivum*). Genome 41: 782–788.

Spielmeyer, W., Moullet, O., Laroche, A. and Lagudah, E. S. 2000. Highly recombinogenic regions at seed storage protein loci on chromosome 1DS of *Aegilops tauschii*, the D-genome donor of wheat. Genetics 155: 361–367.

Suoniemi, A., Anamthawat-Jónsson, K., Arna, T. and Schulman, A.H. 1996a. Retrotransposon *BARE*-1 is a major, dispersed component of the barley (*Hordeum vulgare* L.) genome. Plant Mol. Biol. 30: 1321–1329.

Suoniemi, A., Narvanto, A. and Schulman, A. 1996b. The *BARE*-1 retrotransposon is transcribed in barley from an LTR promoter active in transient assays. Plant Mol. Biol. 31: 295–306.

Sybenga, J. 1996. Recombination and chiasmata: few but intriguing discrepancies. Genome 39: 473–484.

Venter, J.C., Adams, M.D., Myers, E.W., Li, P.W., Mural, R.J. *et al.* 2001. The sequence of the human genome. Science 291: 1304–1351.

Vicient, C.M., Suoniemi, A., Anamthawat-Jónsson, K., Tanskanen, J., Beharav, A., Nevo, E. and Schulman, A.H. 1999. Retrotransposon *BARE*-1 and its role in genome evolution in the genus *Hordeum*. Plant Cell 11: 1769–1784.

Vicient, C.M., Jääskeläinen, M., Kalendar, R. and Schulman, A.H. 2001. Active retrotransposons are a common feature of grass genomes. Plant Physiol. 125: 1283–1292.

Waugh, R., McLean, K., Flavell, A.J., Pearce, S.R., Kumar, A., Thomas, B.B.T. and Powell, W. 1997. Genetic distribution of *BARE*-1-like retrotransposable elements in the barley genome revealed by sequence-specific amplification polymorphisms (S-SAP). Mol. Gen. Genet. 253: 687–694.

Weng, Y., Tuleen, N.A. and Hart, G.E. 2000. Extended physical maps and consensus physical map of the homoeologous group-6 chromosomes of wheat (*Triticum aestivum* L. em Thell.). Theor. Appl. Genet. 100: 519–527.

WGRC home page: http//www.ksu.edu/WGRC

Wicker, T., Stein, N., Albar, L., Feuillet, C., Schlagenhauf, E. and Keller, B. 2001. Analysis of a contiguous 211 kb sequence in diploid wheat (*Triticum monococcum*) reveals multiple mechanisms of genome evolution. Plant J. 26: 307–316.

Yu, A., Zhao, C., Fan, Y., Jang, W., Mungall, A.J., Deloukas, P., Olsen, A., Doggett, N.A., Ghebranious, N., Broman, K.W. and Weber, J.L. 2001. Comparison of human genetic and sequence-based physical maps. Nature 409: 951–953.